Electronic Supporting Information (ESI)

Subtle structural variation in azine/ imine derivatives controls Zn^{2+} sensitivity: ESIPT-CHEF combination for nano-molar detection of Zn^{2+} with DFT support

Somnath Khanra, Sabyasachi Ta, Milan Ghosh, Sudeshna Chatterjee and Debasis Das*

Department of Chemistry, The University of Burdwan, Burdwan, 713104, W.B., India

1. **General method of UV-Vis and fluorescence titration**

Path length of the cells used for absorption and emission studies is 1 cm. For UV-Vis and fluorescence titrations, stock solution of **L1**, **L2**, **L3** and **L4** is prepared (20 μM) in bis-tris buffer solution (5 mM), pH 7.4, DMSO/H_2O (1:1, v/v). Working solutions of **L1**, **L2**, **L3** and **L4**, and **Zn^{2+}** are prepared from their respective stock solutions. Fluorescence measurements have been performed using 5 nm x 5 nm slit width.

2. **Job's plot from fluorescence experiment.**

A series of solutions containing **L1**, **L2**, **L3** and **L4** and **Zn^{2+}** are prepared such that the total concentration of **Zn^{2+}** and **L1**, **L2**, **L3** and **L4** remained constant (20 μM) in all the sets. The mole fraction (**x**) of **Zn^{2+}** is varied from 0.1 to 0.9. The fluorescence intensity of **zinc adduct** is plotted respectively against the mole fraction of **Zn^{2+}**.

3. Determination of Binding constant:

The binding constants of adduct for different analyte are determined using the following Benesi-Hildebrand equation[1].

$$\frac{F_{max} - F_{min}}{F_X - F_{min}} = 1 + \frac{1}{K[C]^n}$$

Where $\mathbf{F_{min}}$, $\mathbf{F_x}$, and $\mathbf{F_{max}}$ are the respective emission intensities of the probe in absence of analyte, at an intermediate analyte concentration, and at a concentration of complete interaction with analyte respectively. **K** is the binding constant, **C** is the concentration of analyte and **n** is the number of analyte bound per probe molecule. The value of **K** are obtained from the slopes of different plot for different probe.

4. Calculation of detection limit

The detection limit (**DL**) is determined from the following equation[2]:

$$DL = \frac{3\sigma}{S}$$

σ is the standard deviation of the blank solution, **S** is the slope of the calibration curve.

Reference:

1. H. A. Benesi and J. H. Hildebrand, *J. Am. Chem. Soc.*, 1949, **71**, 2703.

2. M. Zhu, M. Yuan, X. Liu, J. Xu, J. Lv, C. Huang, H. Liu, Y. Li, S. Wang, D. Zhu, *Org. Lett.*, 2008, **10**, 1481.

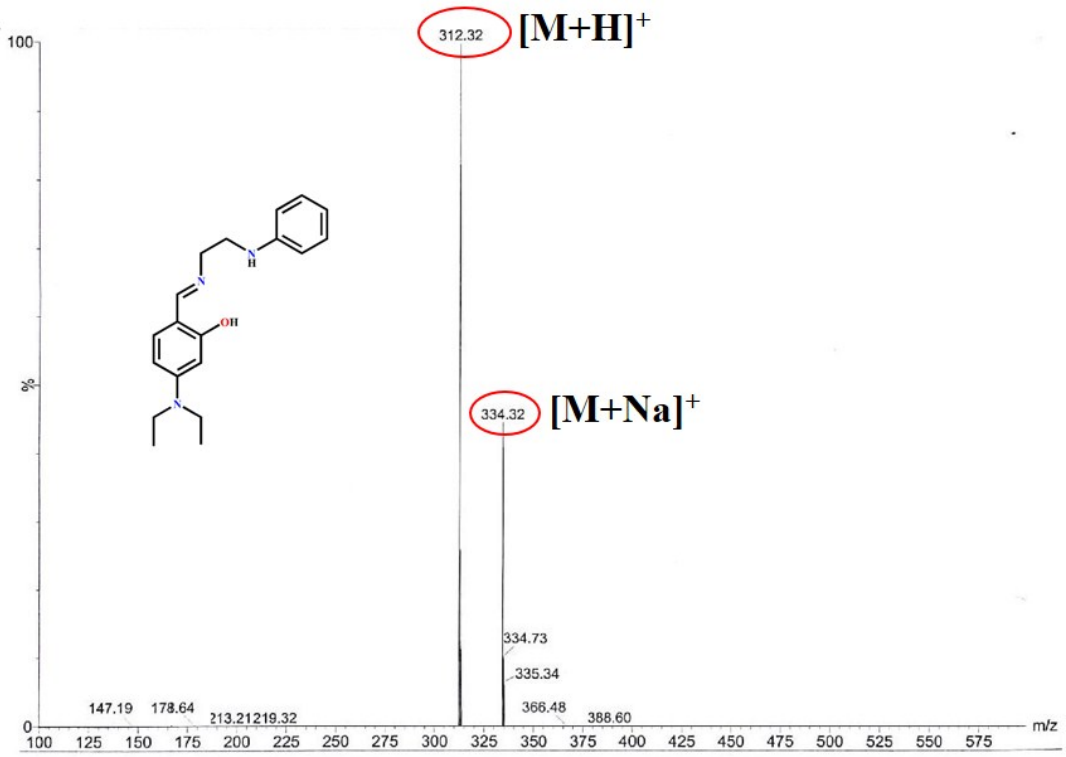

Figure S1a QTOF mass spectrum of **L1**.

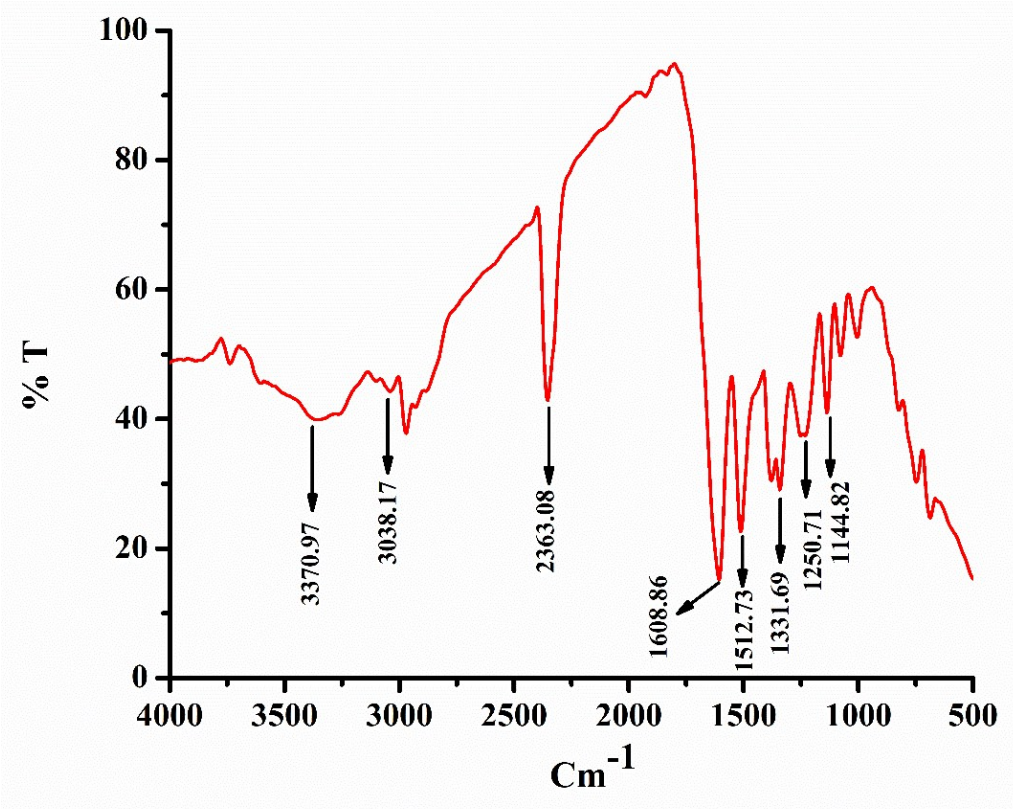

Figure S1b FTIR spectrum of compound **L1**

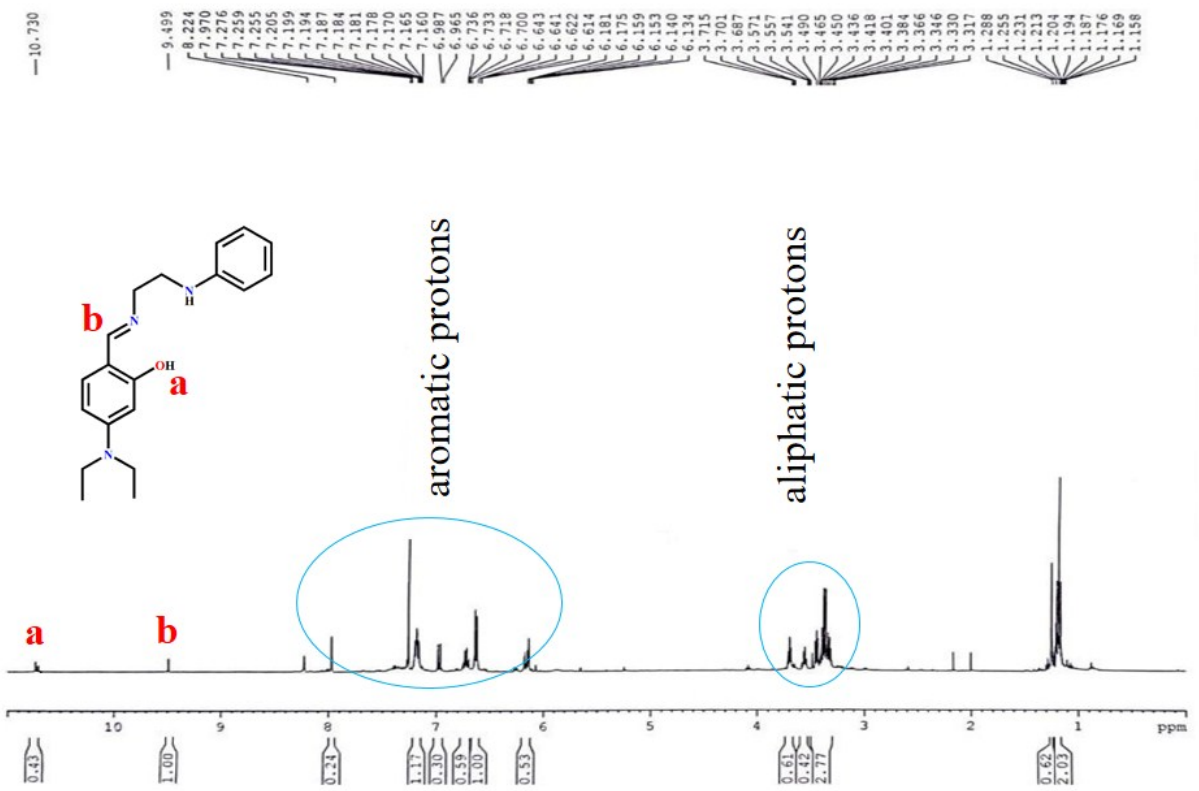

Figure S1c ^{1}H-NMR spectrum of **L1** in $CDCl_3$

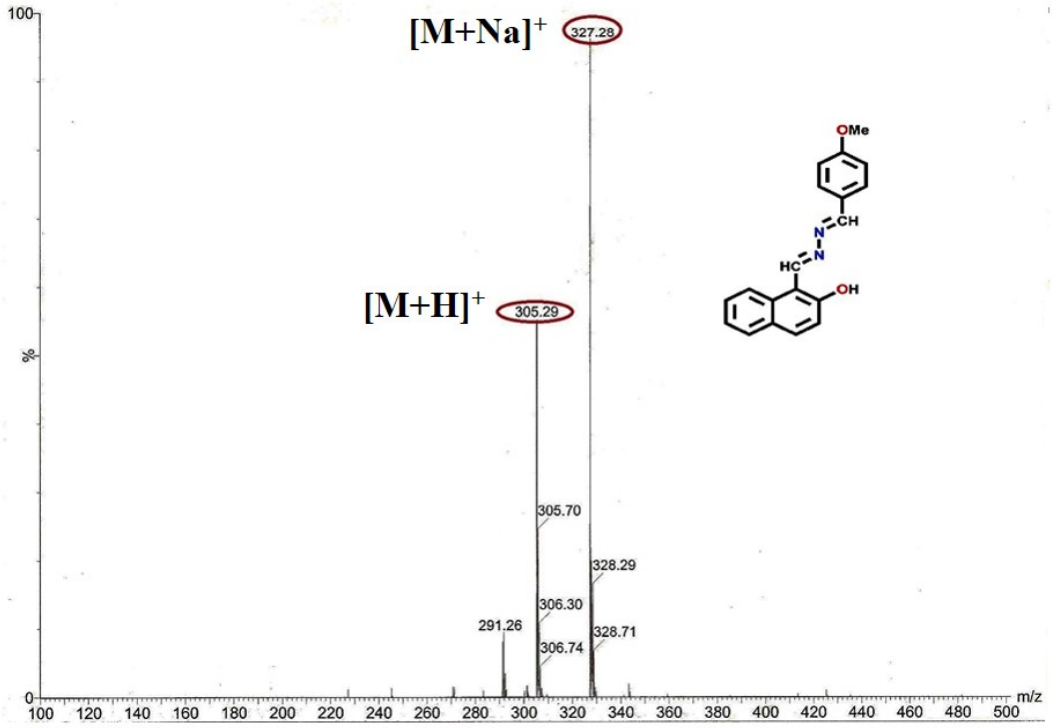

Figure S2a QTOF mass spectrum of **L2**.

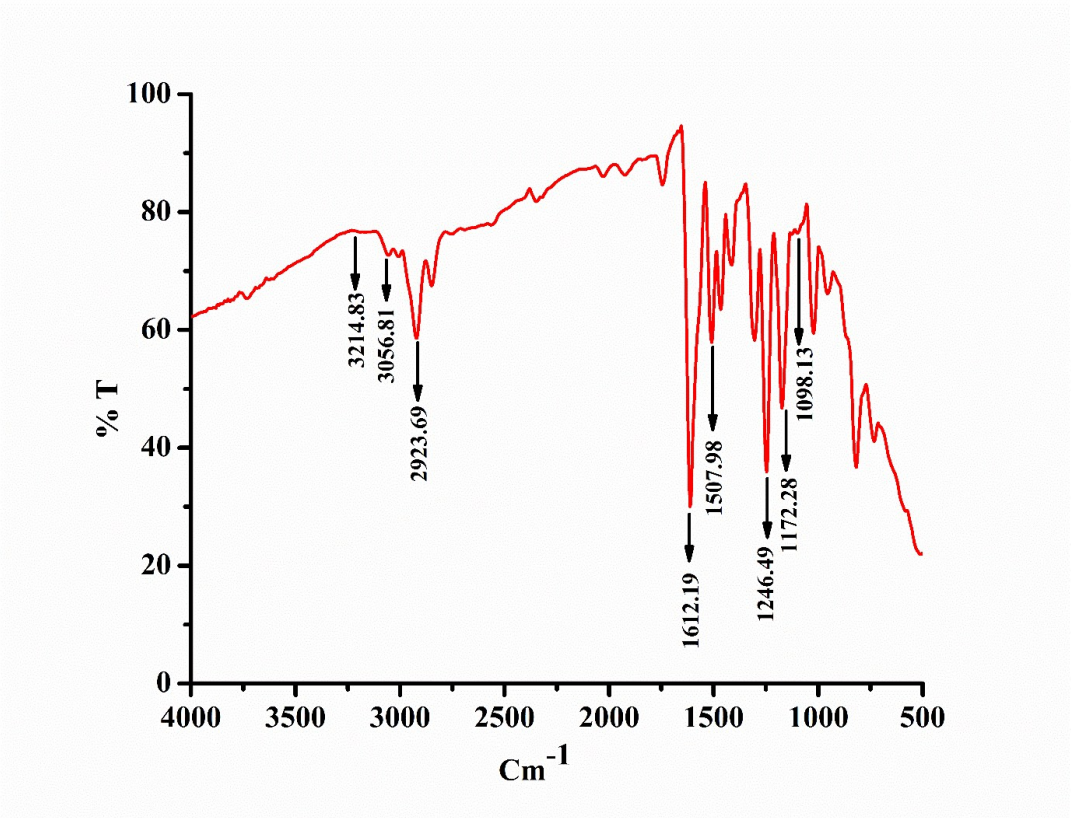

Figure S2b FTIR spectrum of compound **L2**

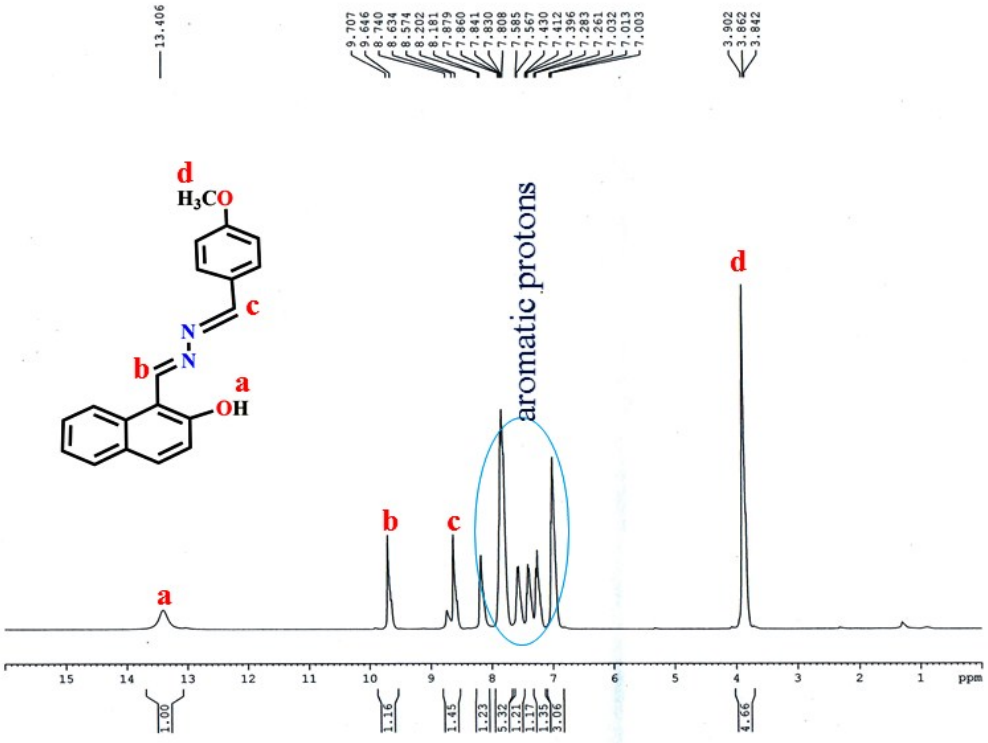

Figure S2c ^{1}H-NMR spectrum of **L2** in $CDCl_3$

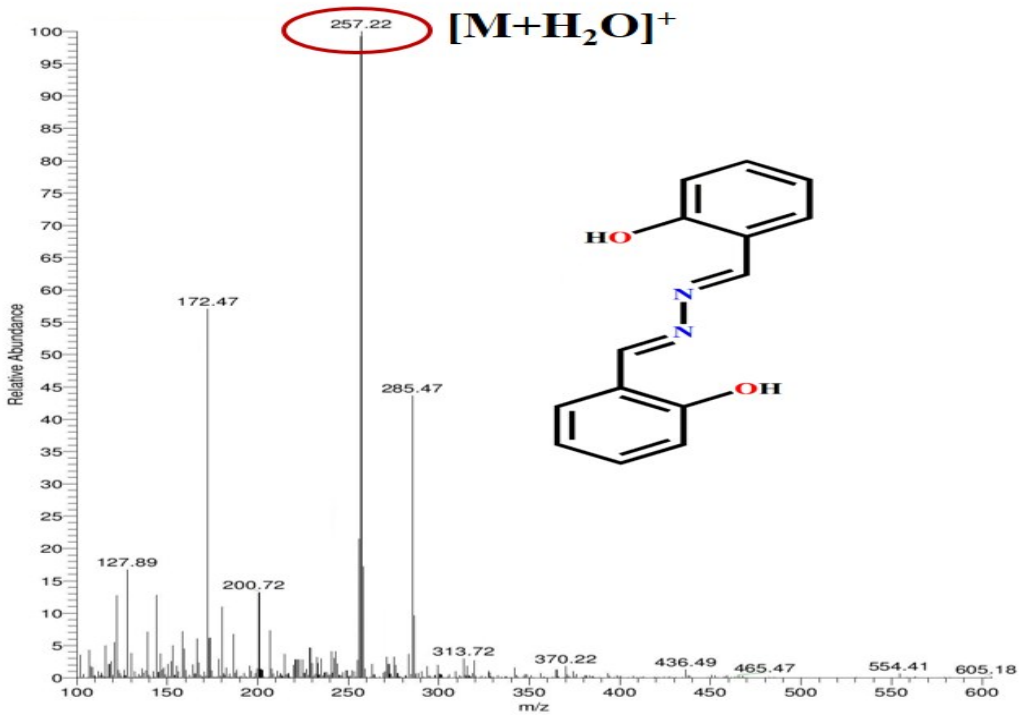

Figure S3a QTOF mass spectrum of **L3**.

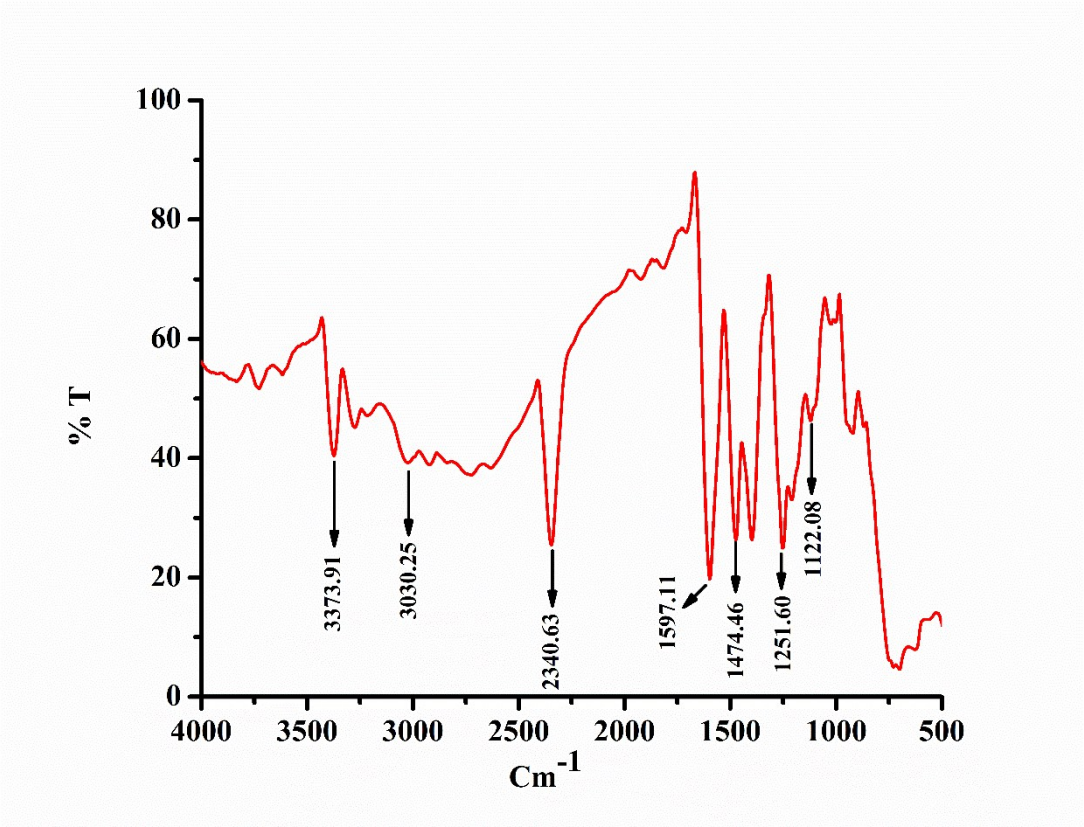

Figure S3b FTIR spectrum of compound **L3**

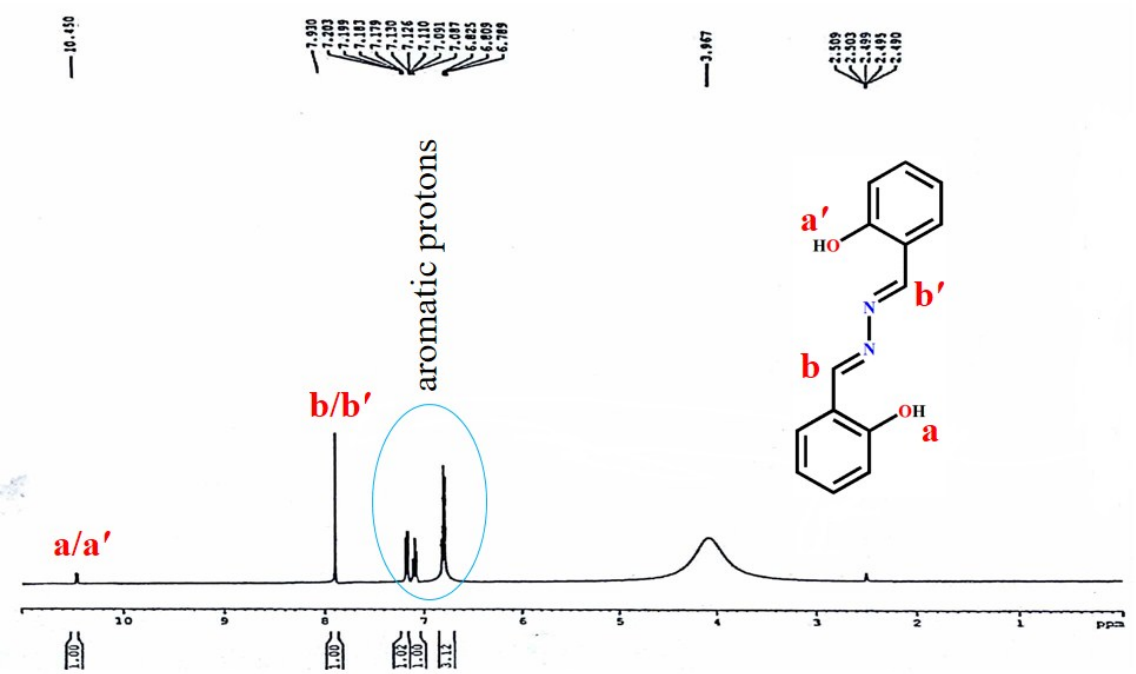

Figure S3c ^{1}H-NMR spectrum of **L3** in DMSO-d_6

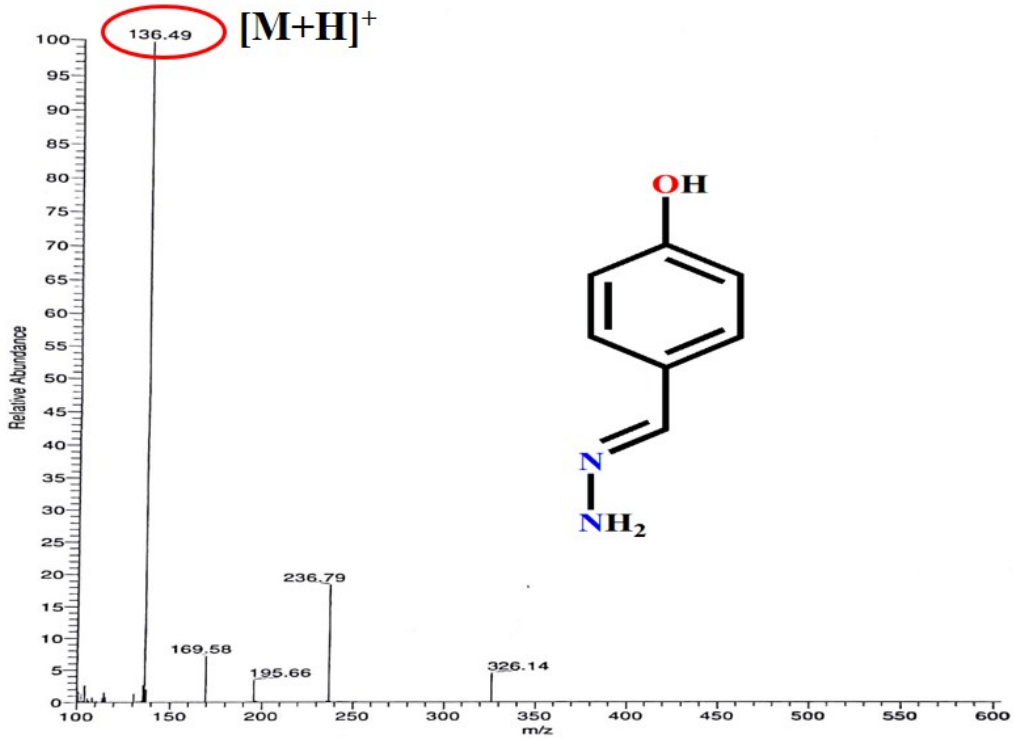

Figure S4a QTOF mass spectrum of **L4a**.

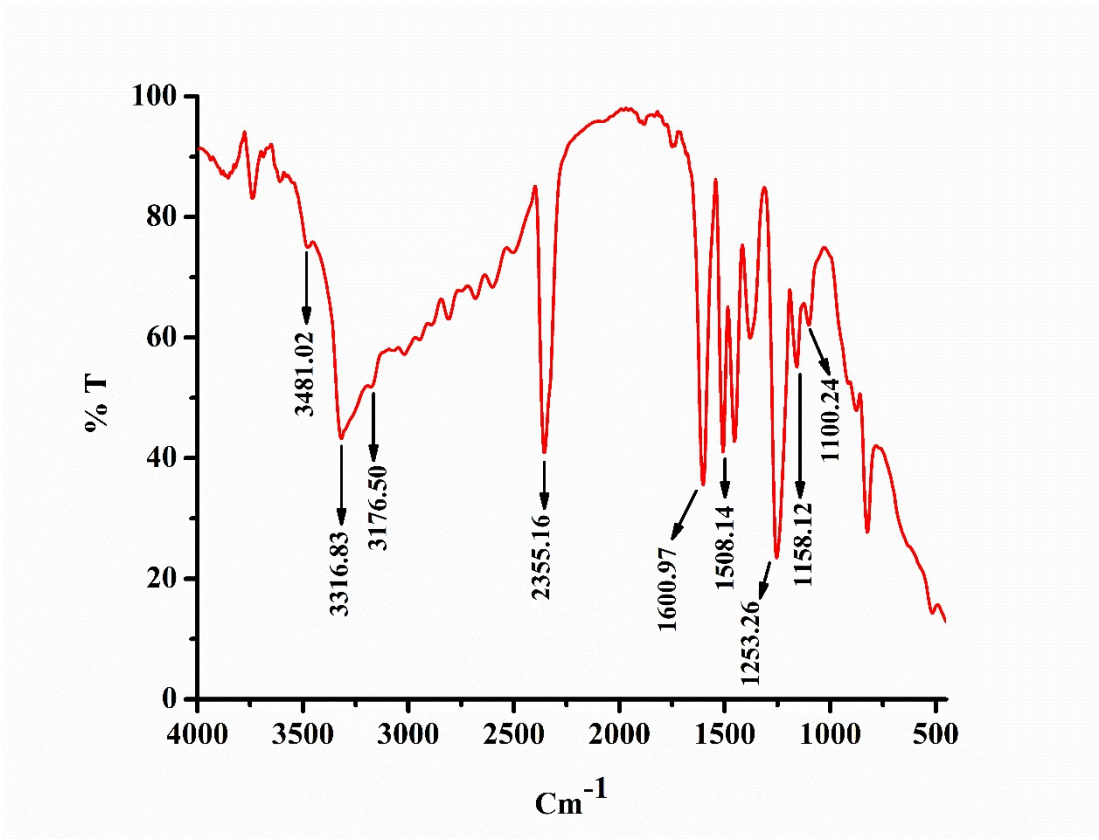

Figure S4b FTIR spectrum of compound **L4a**

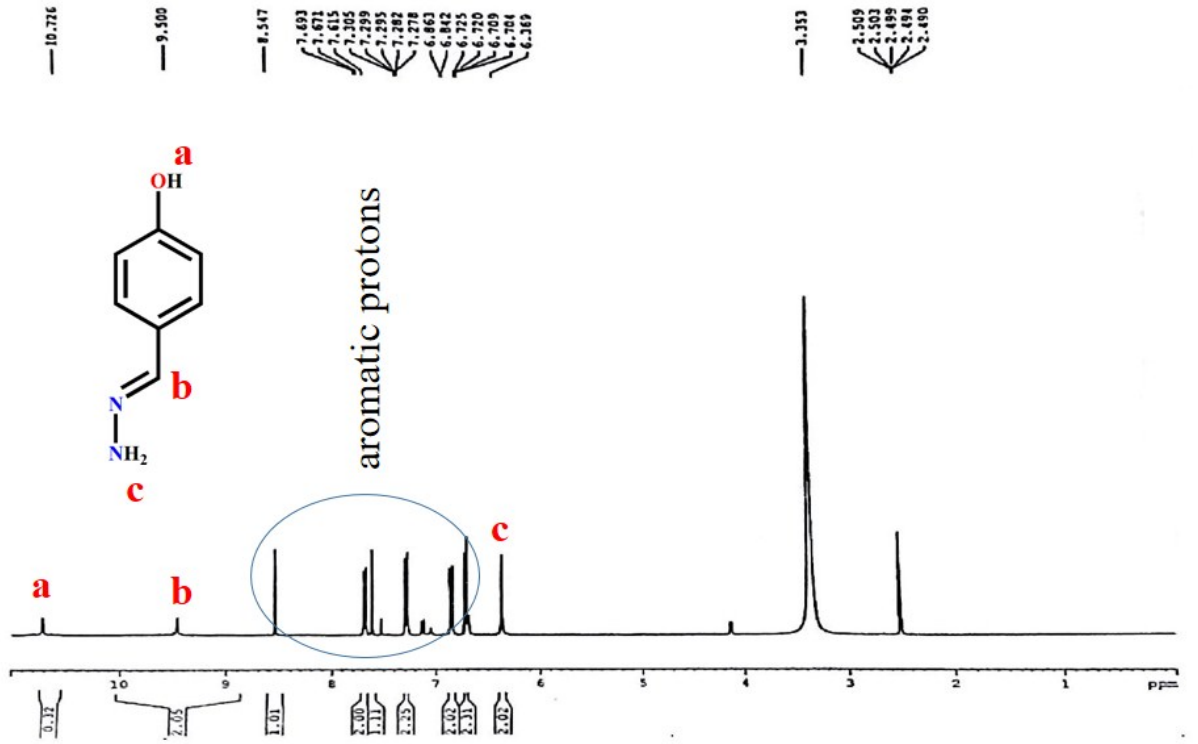

Figure S4c ^{1}H-NMR spectrum of **L4a** in DMSO-d_6

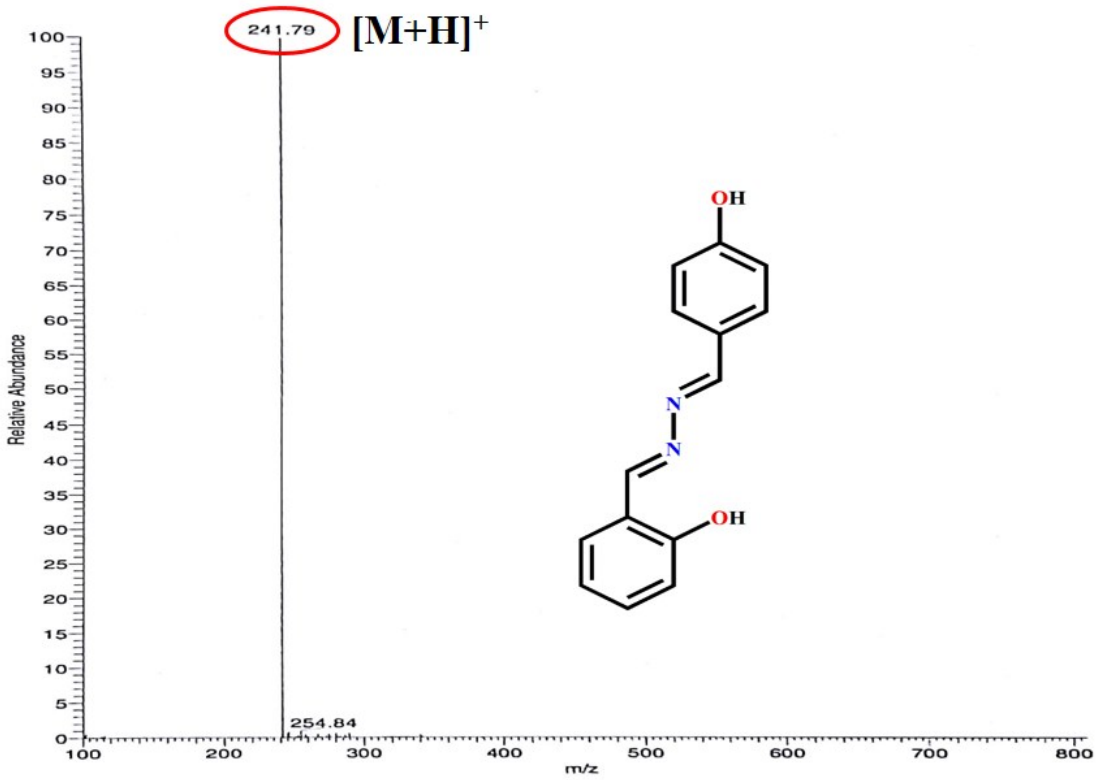

Figure S4d QTOF mass spectrum of **L4**.

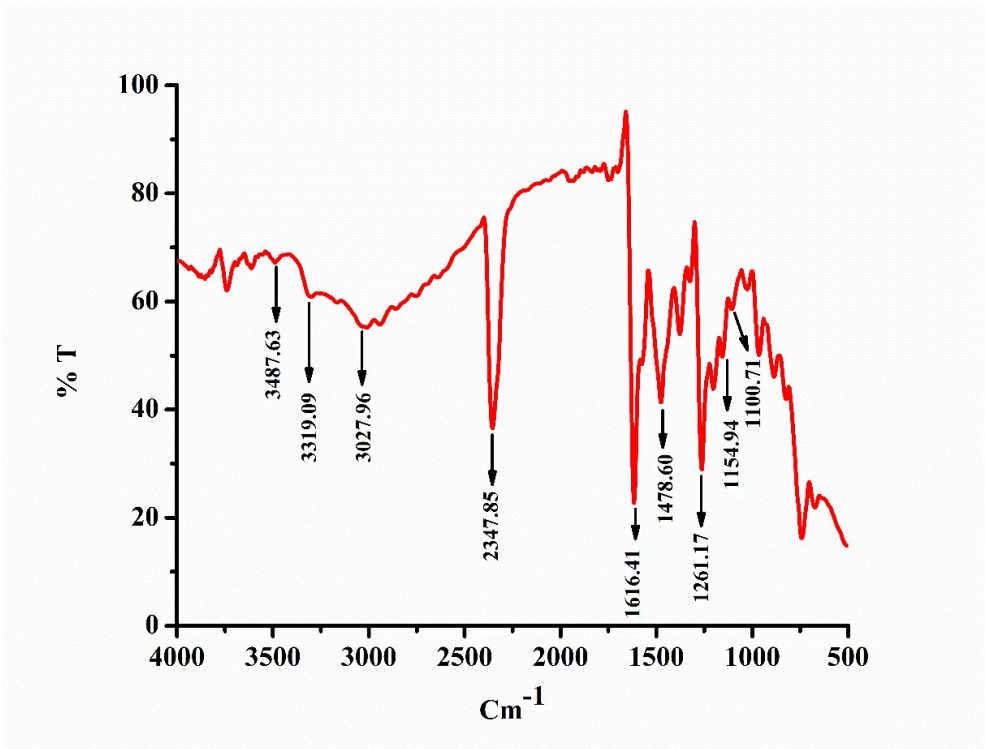

Figure S4e FTIR spectrum of compound **L4**

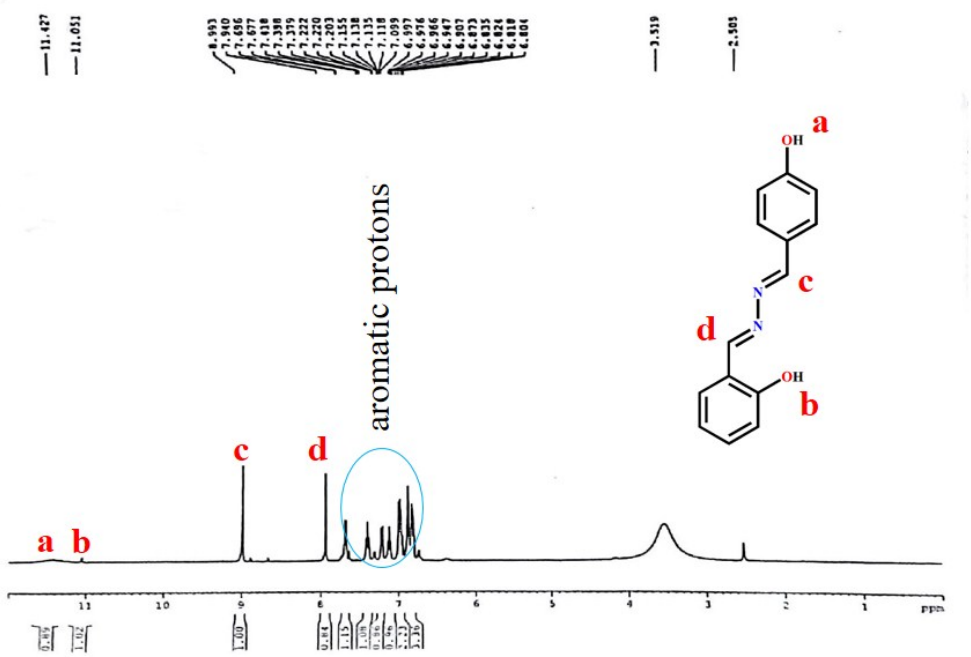

Figure S4f ^{1}H-NMR spectrum of **L4** in DMSO-d_6

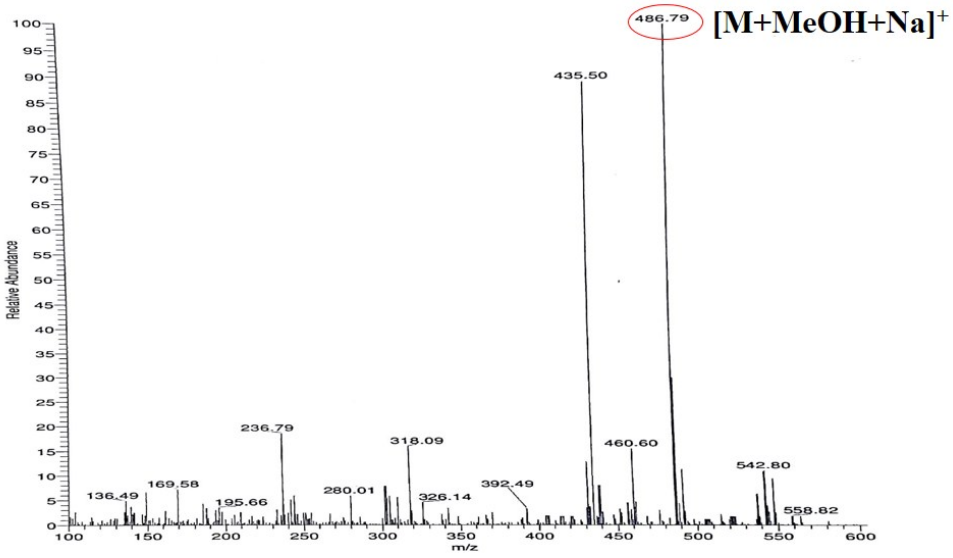

Figure S5a TOF mass spectrum of **Ad1**.

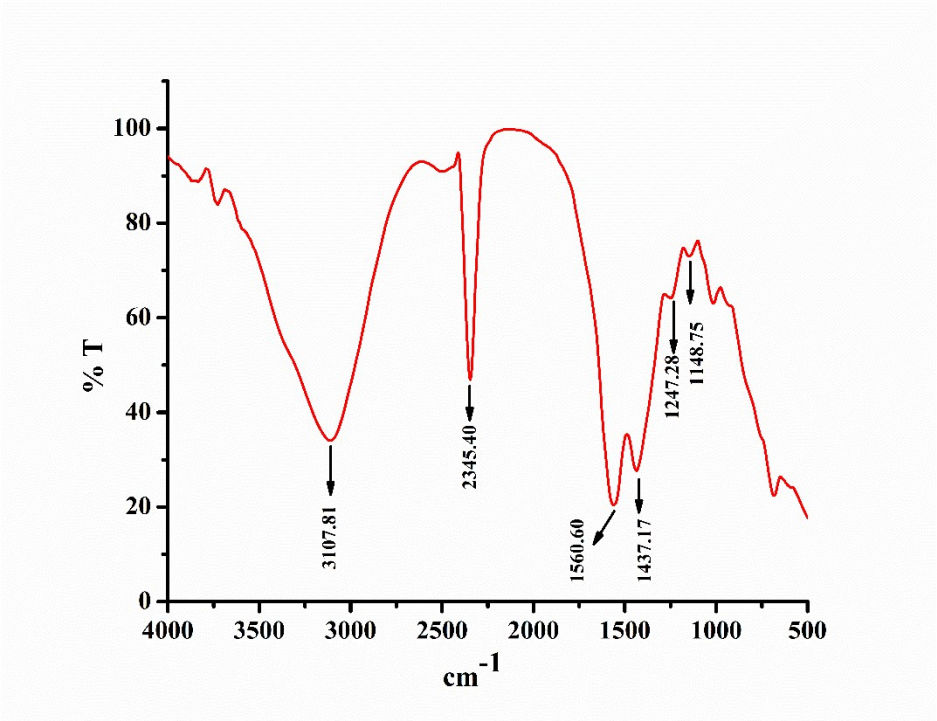

Figure S5b FTIR spectrum of compound **Ad1**

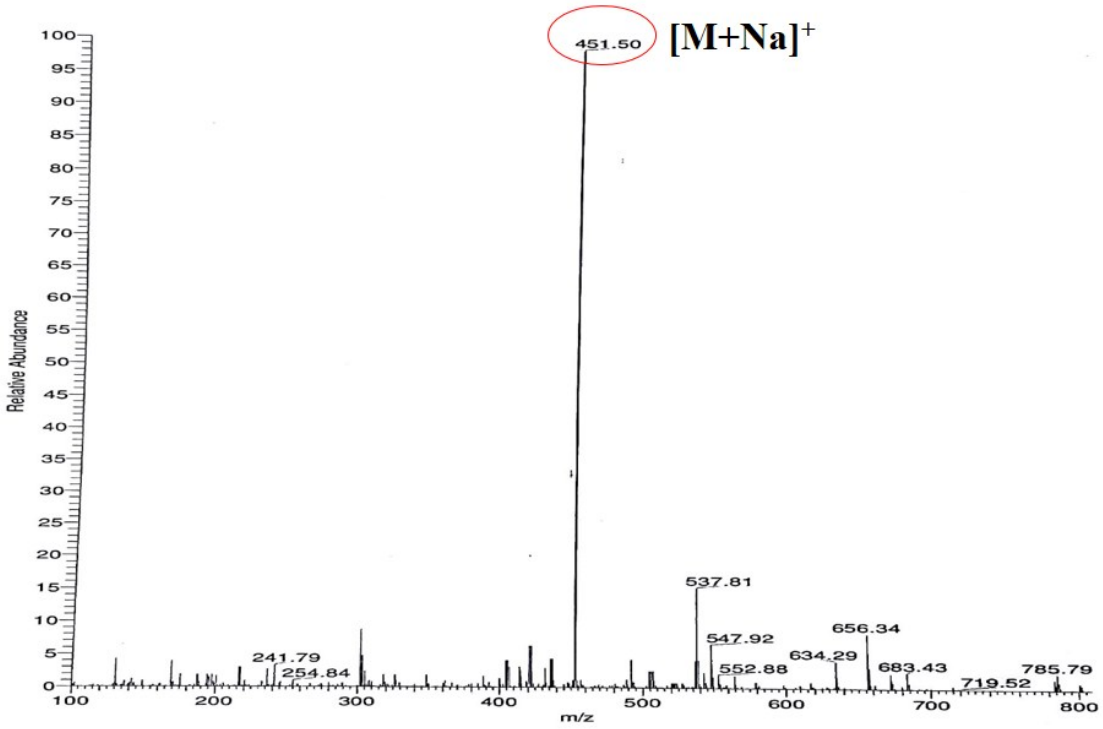

Figure S6a QTOF mass spectrum of **Ad2**.

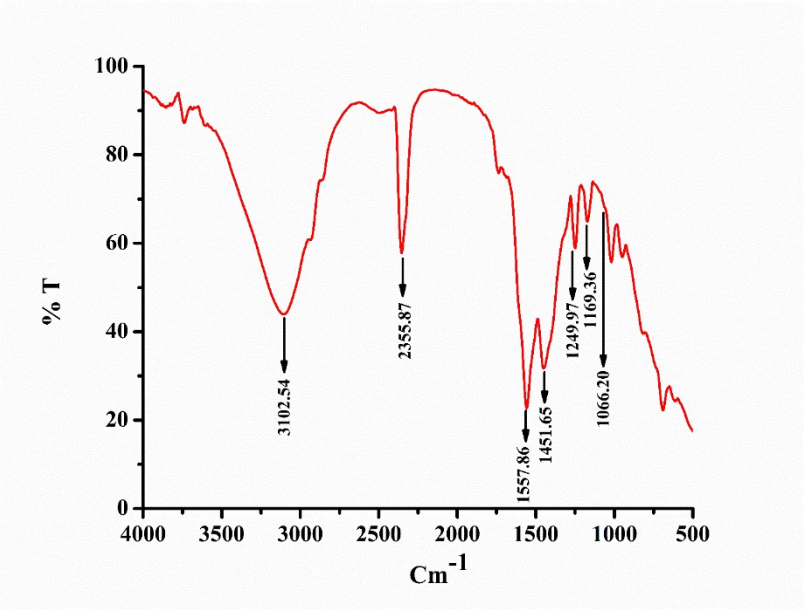

Figure S6b FTIR spectrum of compound **Ad2**

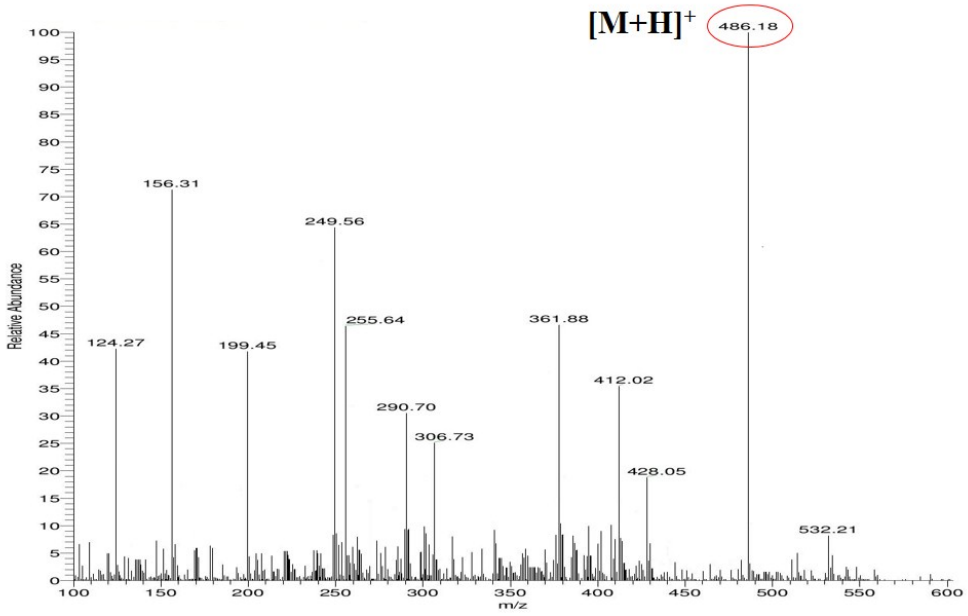

Figure S7a QTOF mass spectrum of **Ad3**.

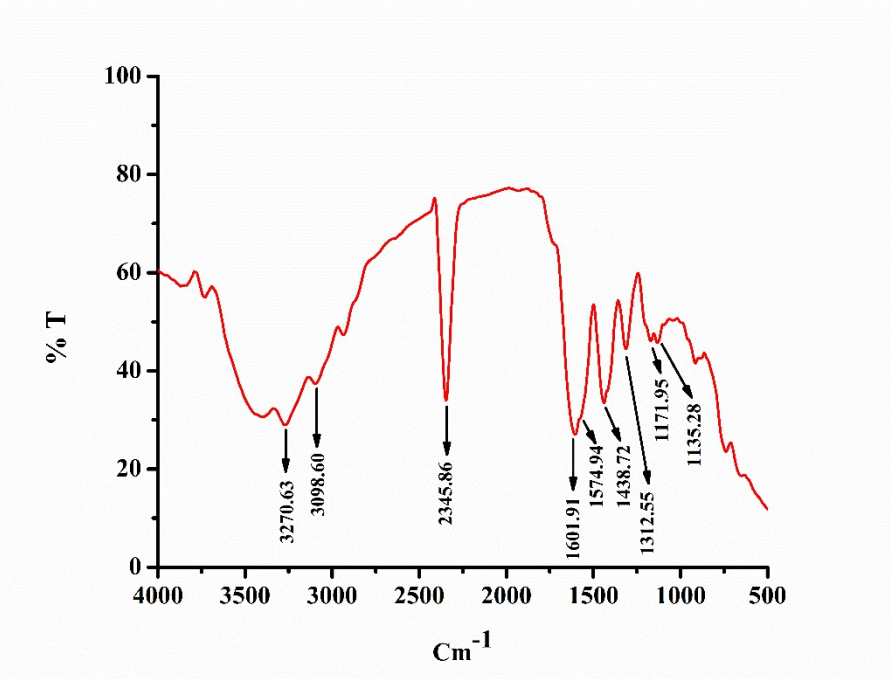

Figure S7b FTIR spectrum of compound **Ad3**

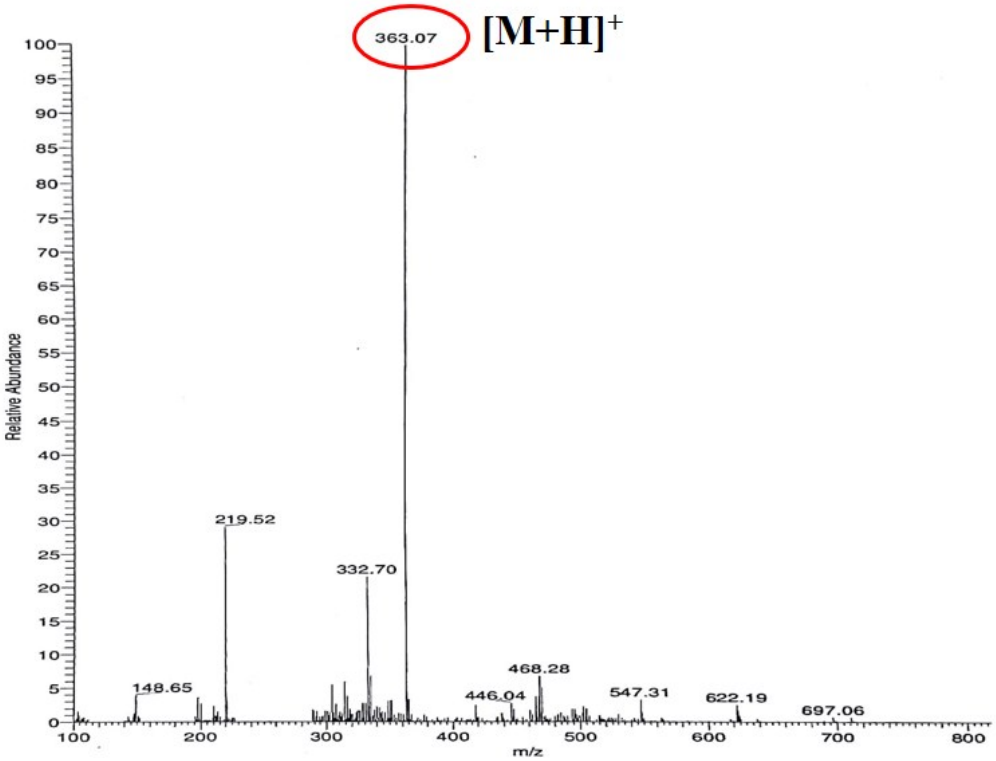

Figure S8a QTOF mass spectrum of **Ad4**.

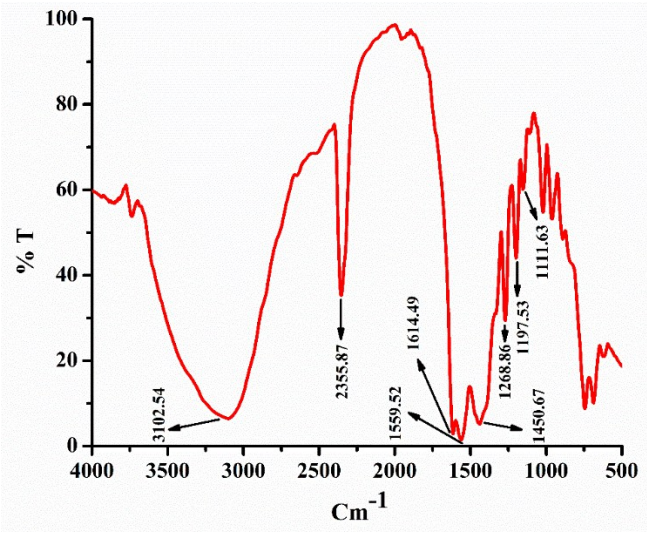

Figure S8b FTIR spectrum of compound **Ad4**

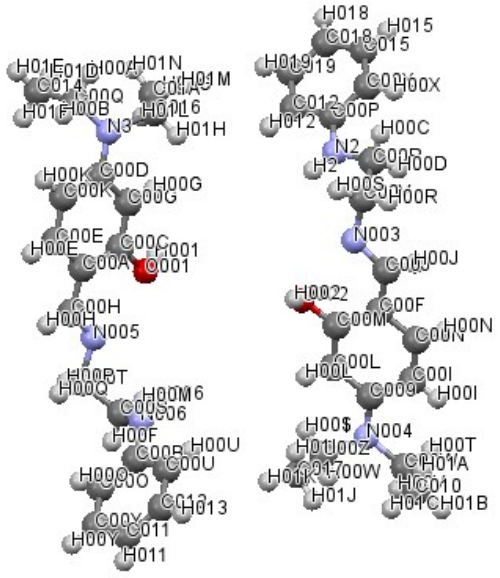

Figure S9a X-ray crystal structure of compound **L1**

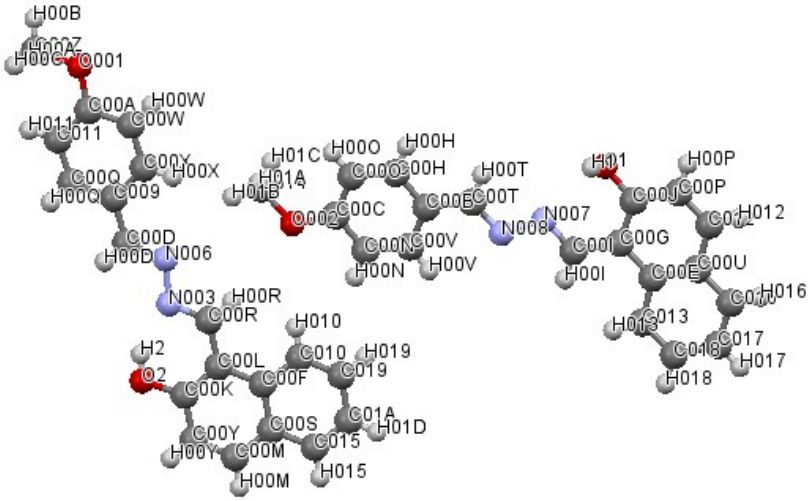

Figure S9b X-ray crystal structure of compound **L2**

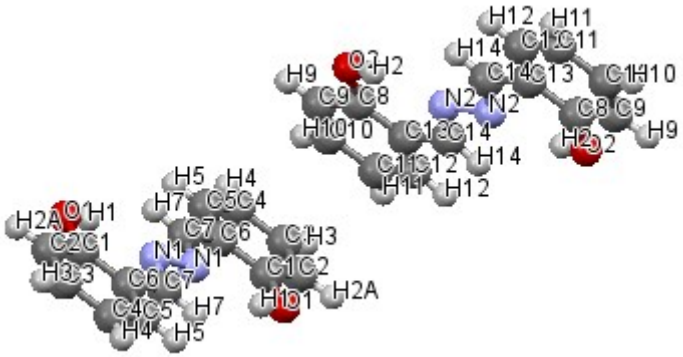

Figure S9c X-ray crystal structure of compound **L3**

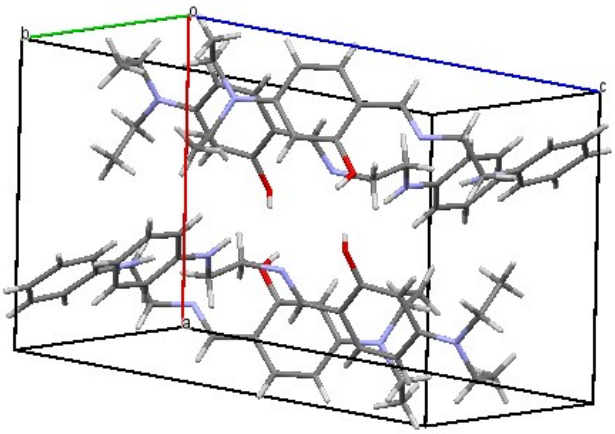

Figure S10a Packing pattern of **L1**

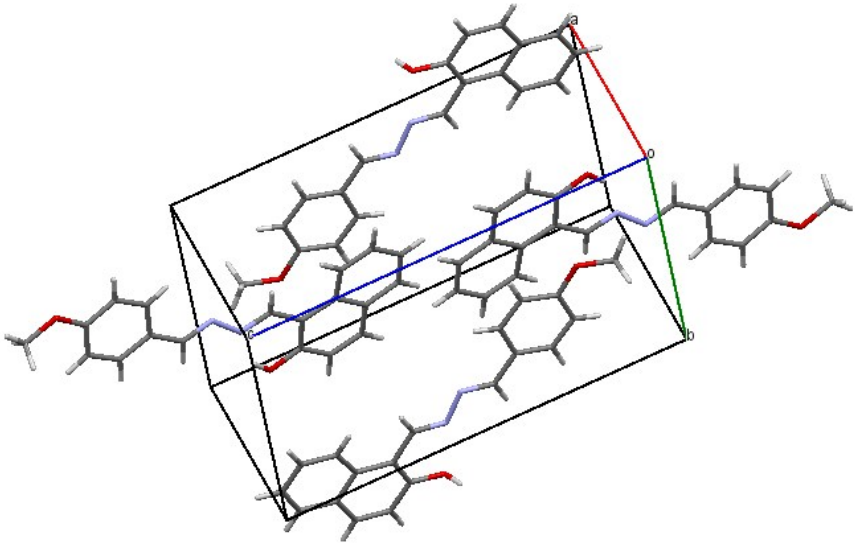

Figure S10b Packing pattern of **L2**

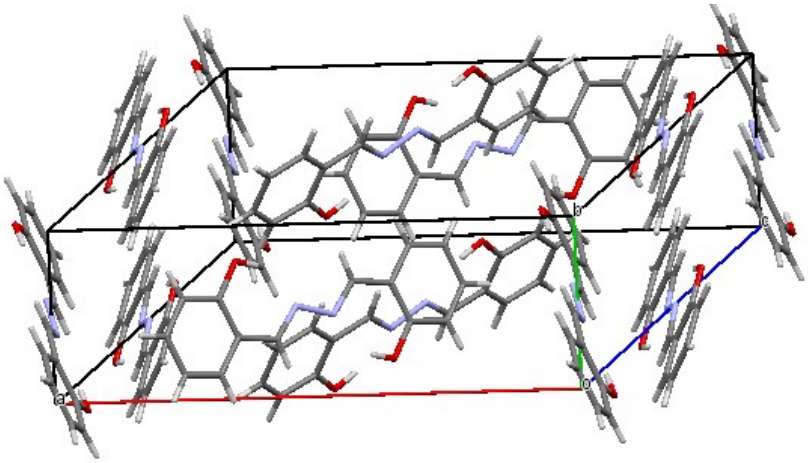

Figure S10c Packing pattern of **L3**

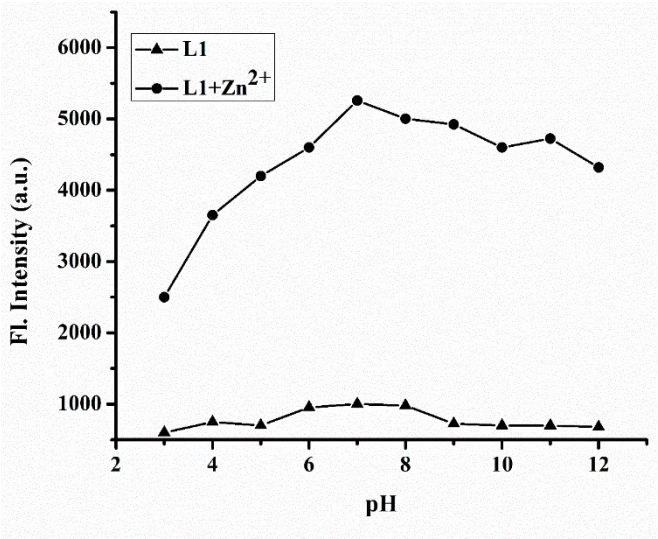

Figure S11a Effect of pH on the emission intensities of compound **L1, (**λ_{ex} = 287 nm, λ_{em} = 414nm) in presence and absence of Zn^{2+}.

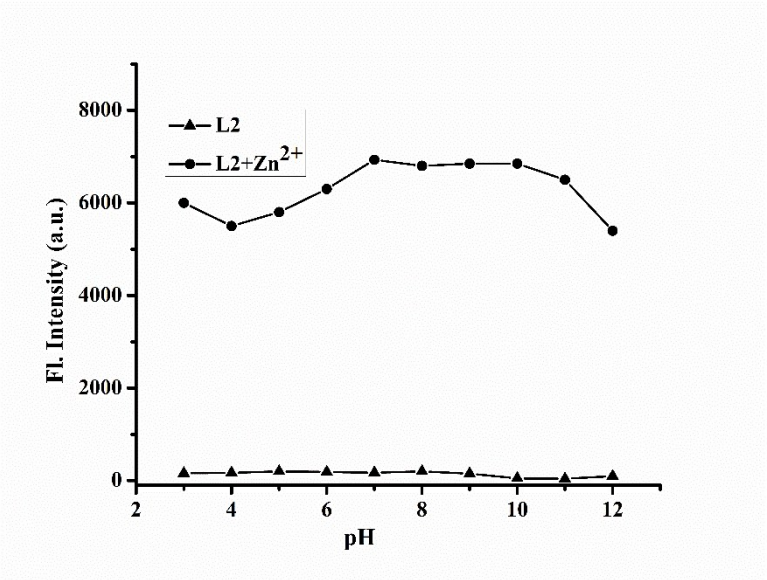

Figure S11b Effect of pH on the emission intensities of compound **L2, (**λ_{ex} = 436 nm λ_{em} = 491 nm) in presence and absence of Zn^{2+}

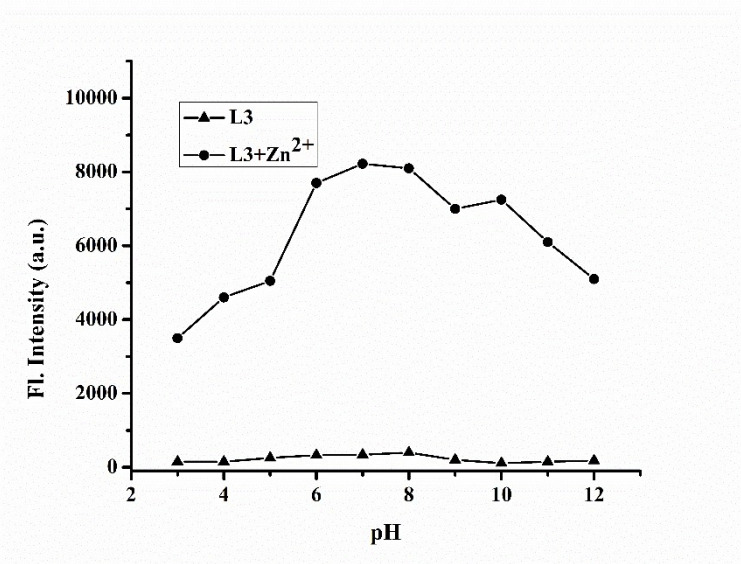

Figure S11c Effect of pH on the emission intensities of compound **L3,** (λ_{ex} = 353 nm λ_{em} = 432 nm) in presence and absence of Zn^{2+}

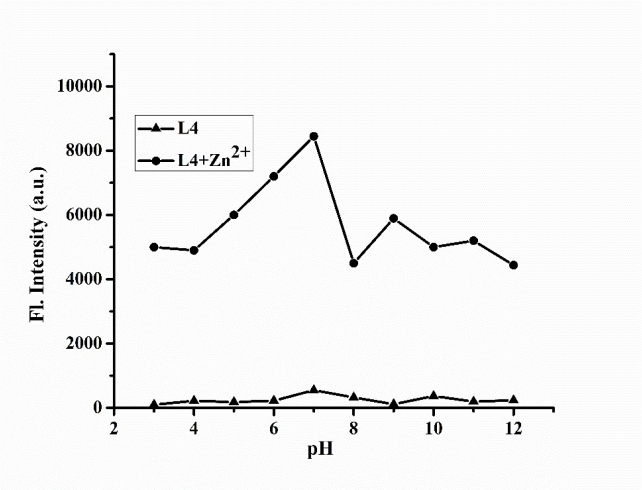

Figure S11d Effect of pH on the emission intensities of compound **L4,** (λ_{ex} = 400 nm λ_{em} = 495 nm) in presence and absence of Zn^{2+}

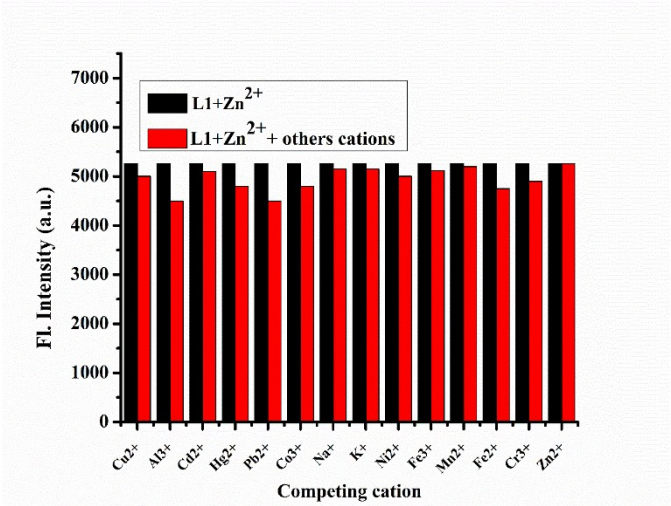

Figure S12a Interference plots (cations) of **L1** for Zn^{2+} in fluorescence (λ_{ex} = 287 nm, λ_{em} = 414 nm)

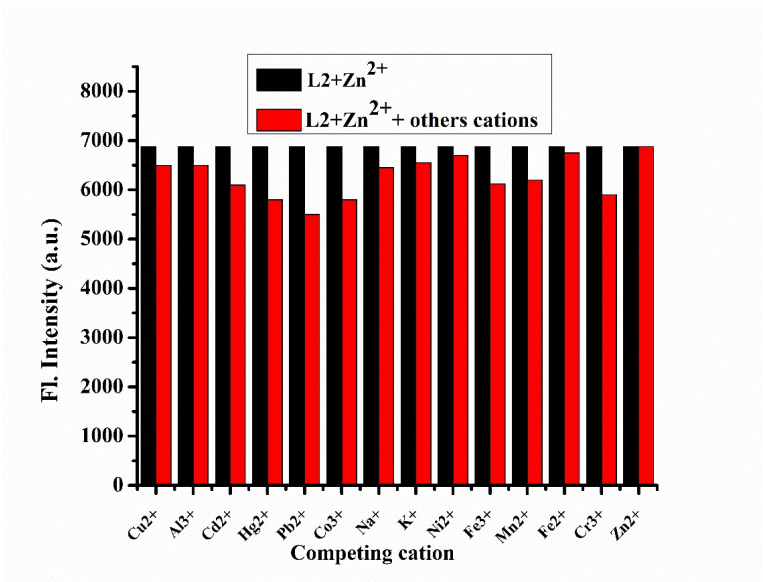

Figure S12b Interference plots (cations) of **L2** for Zn^{2+} in fluorescence (λ_{ex} = 436 nm, λ_{em} = 491 nm)

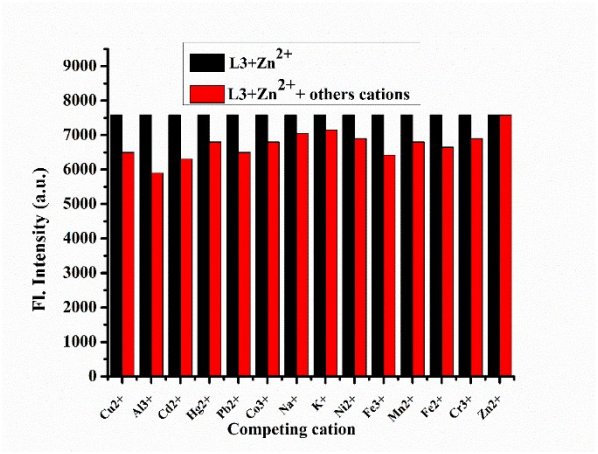

Figure S12c Interference plots (cations) of **L3** for Zn^{2+} in fluorescence (λ_{ex} = 353 nm, λ_{em} = 432 nm)

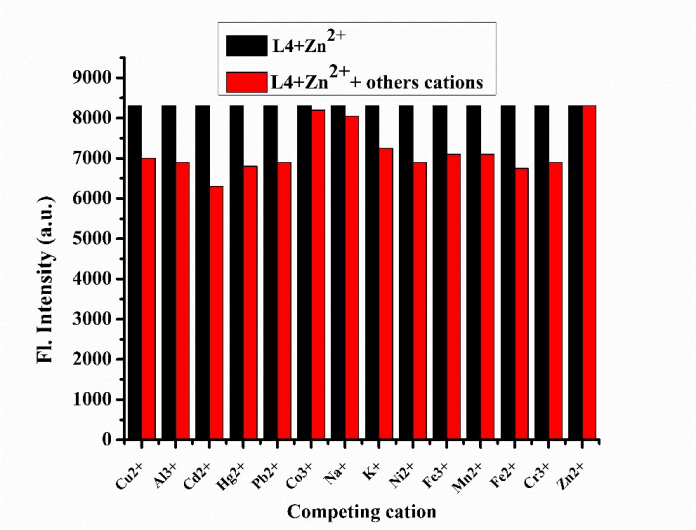

Figure S12d Interference plots (cations) of **L4** for Zn^{2+} in fluorescence (λ_{ex} = 400 nm, λ_{em} = 495 nm)

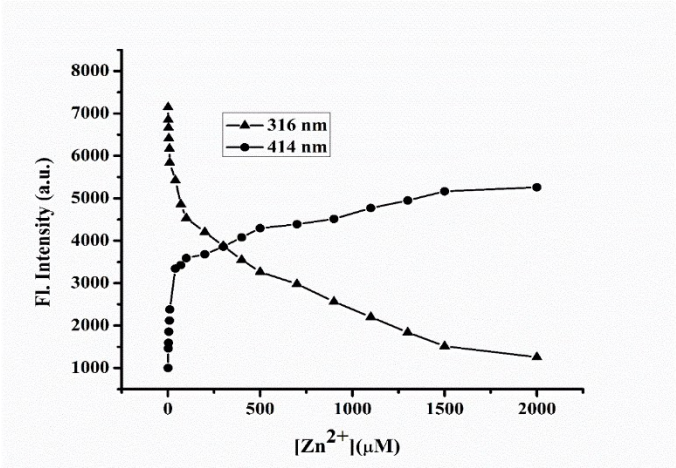

Figure S13a Plot of emission intensities of **L1** (20 μM, λ_{ex} = 287 nm, λ_{em} = 316 nm and 414 nm) as a function of externally added $\mathbf{Zn^{2+}}$ (1.0-2000 μM)

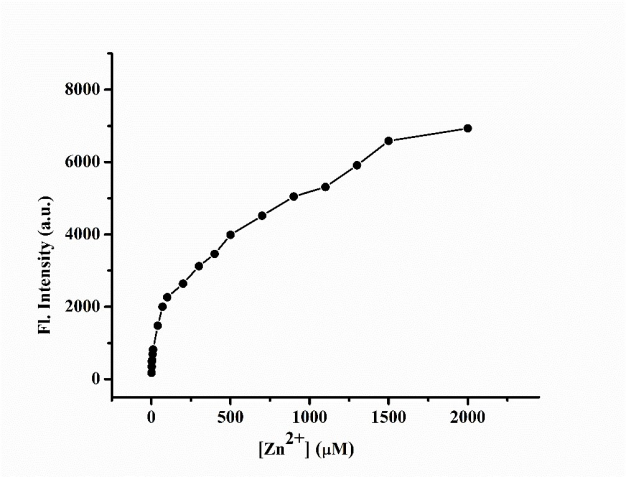

Figure S13b Plot of emission intensities of **L2** (20 μM, λ_{ex} = 436 nm, λ_{em} = 491 nm) as a function of externally added $\mathbf{Zn^{2+}}$ (1.0-2000 μM)

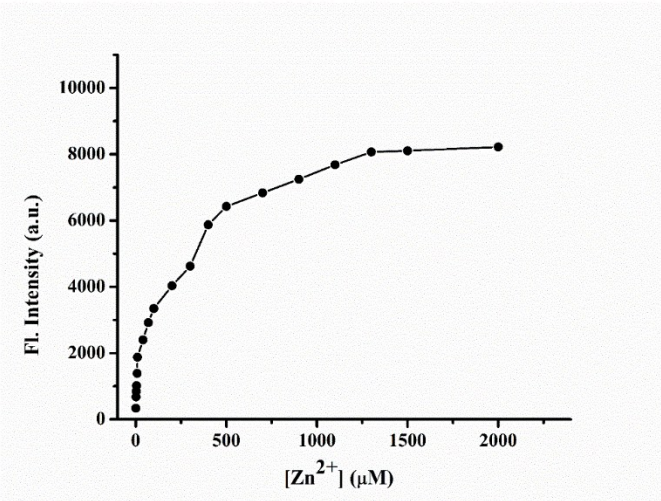

Figure S13c Plot of emission intensities of **L3** (20 μM, λ_{ex} = 353 nm, λ_{em} = 432 nm) as a function of externally added $\mathbf{Zn^{2+}}$ (1.0-2000 μM)

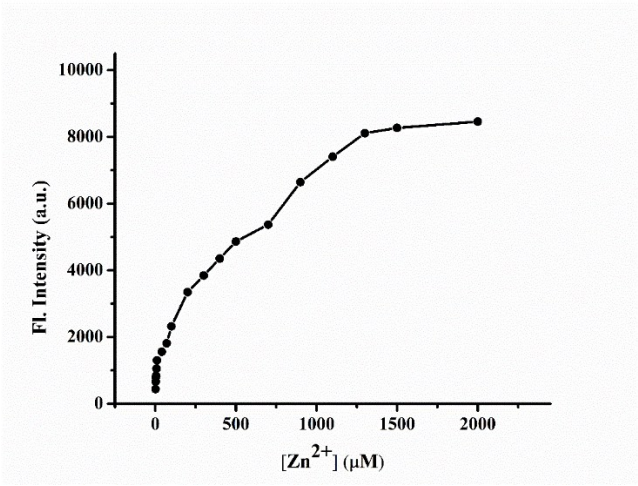

Figure S13d Plot of emission intensities of **L4** (20 μM, λ_{ex} = 400 nm, λ_{em} = 495 nm) as a function of externally added Zn^{2+} (1.0-2000 μM)

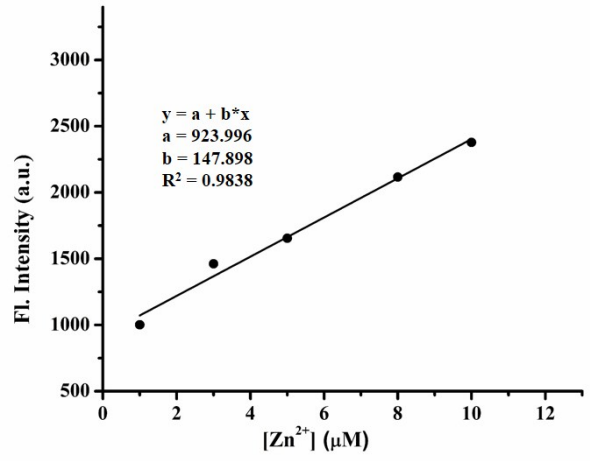

Figure S14a Determination of the detection limit based on change in the ratio (λ_{ex} = 287 nm, λ_{em} = 414 nm) of **L1** (20 μM) with Zn^{2+}, linier portion of **figure S13a** at 414 nm

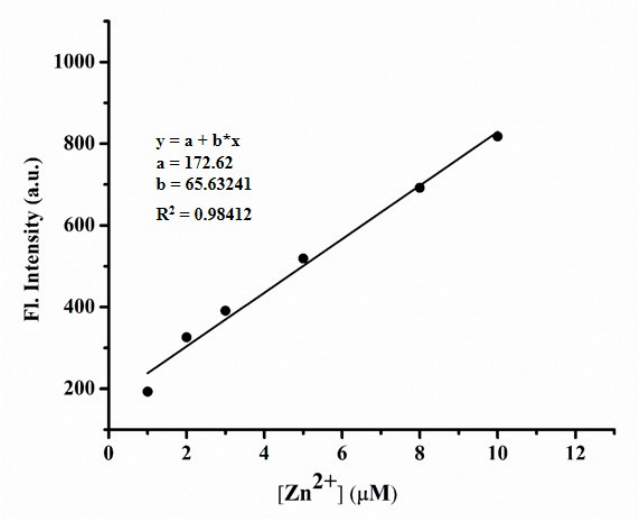

Figure S14b Determination of the detection limit based on change in the ratio (λ_{ex} = 436 nm, λ_{em} = 491 nm) of **L2** (20 μM) with Zn^{2+}, linier portion of **figure S13b**

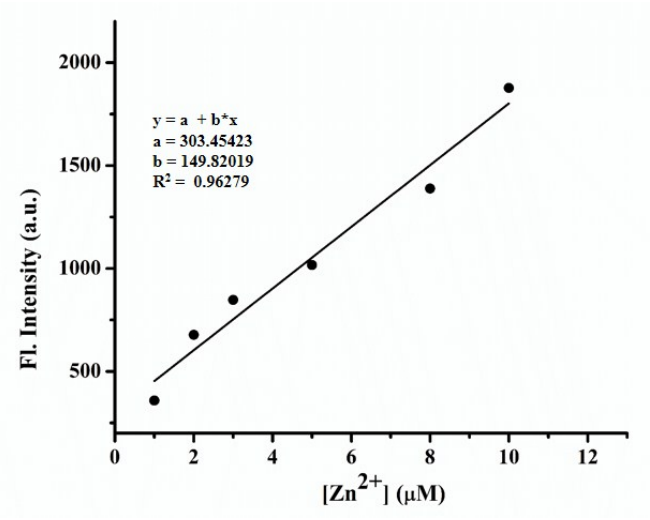

Figure S14c Determination of the detection limit based on change in the ratio (λ_{ex} = 353 nm, λ_{em} = 432 nm) of **L3** (20 μM) with Zn^{2+}, linier portion of **figure S13c.**

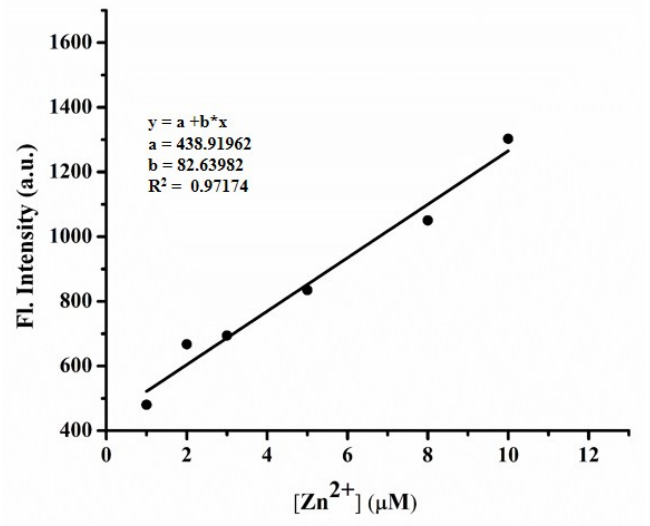

Figure S14d Determination of the detection limit based on change in the ratio (λ_{ex} = 400 nm, λ_{em} = 495 nm) of **L4** (20 μM) with Zn^{2+}, linier portion of **figure S13d**.

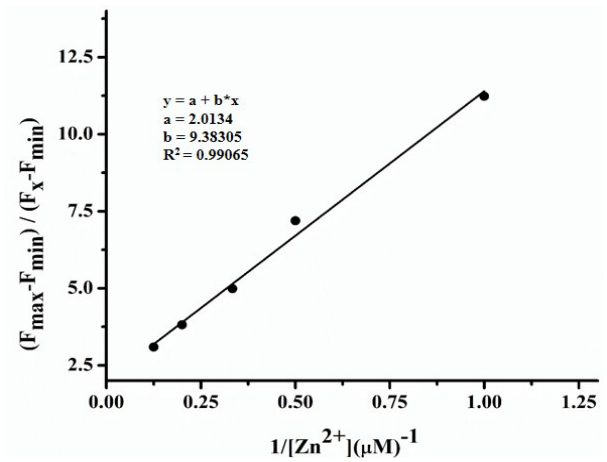

Figure S15a Benesi−Hildebrand plot for determination of association constant of compound **L1** with Zn^{2+} (linier portion only), λ_{ex} = 287 nm, λ_{em} = 414nm.

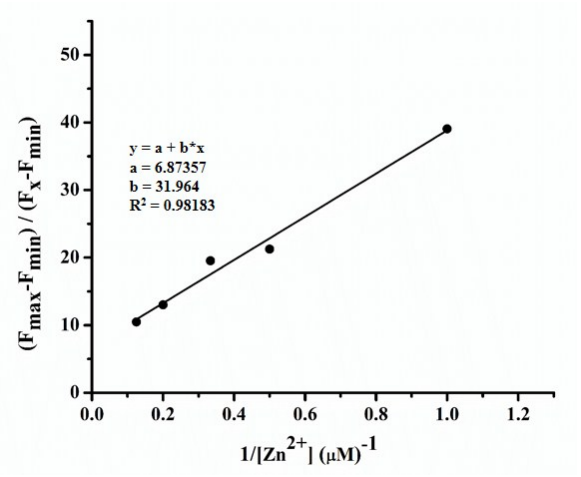

Figure S15b Benesi−Hildebrand plot for determination of association constant of compound **L2** with Zn^{2+} (linier portion only), λ_{ex} = 436 nm, λ_{em} = 491 nm.

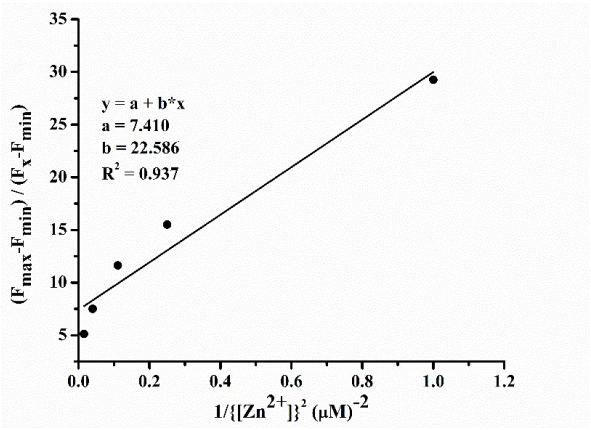

Figure S15c Benesi−Hildebrand plot for determination of association constant of compound **L3** with Zn^{2+} (linier portion only), λ_{ex} = 353 nm, λ_{em} = 432 nm

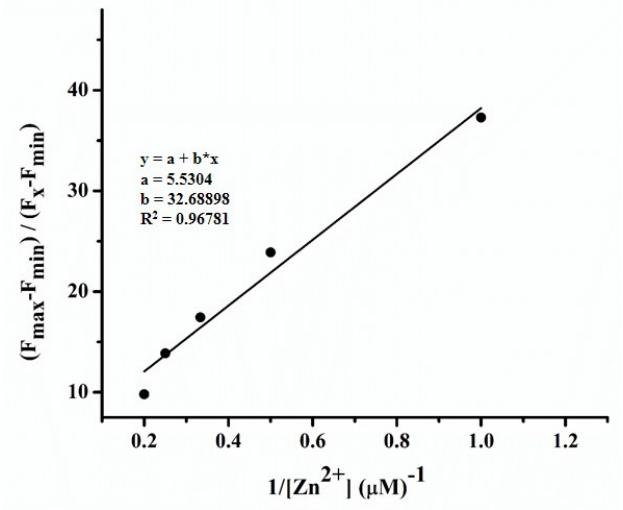

Figure S15d Benesi−Hildebrand plot for determination of association constant of compound **L3** with Zn^{2+} (linier portion only), λ_{ex} = 400 nm, λ_{ex} = 495 nm

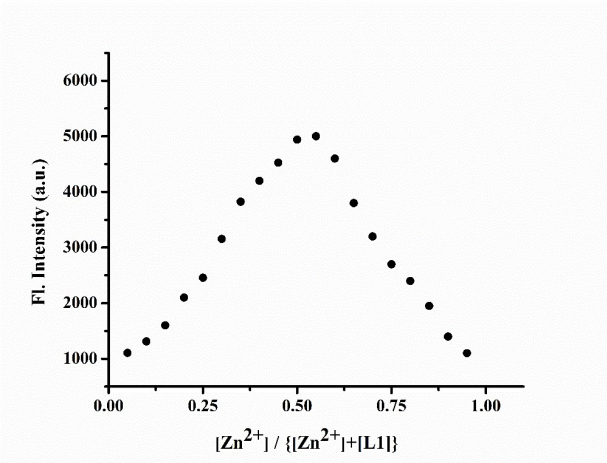

Figure S16a Job's plot for stoichiometry determination of **[L1-Zn^{2+}]** complex**,** (λ_{ex} = 287 nm λ_{em} = 414 nm)

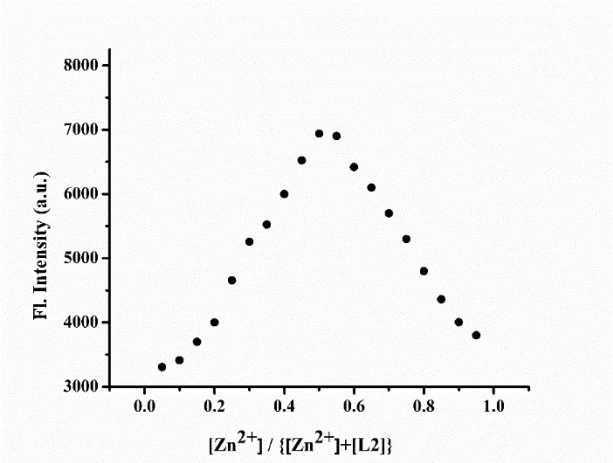

Figure S16b Job's plot for stoichiometry determination of **[L2-Zn^{2+}]** complex, (λ_{ex} = 436 nm λ_{em} = 491 nm)

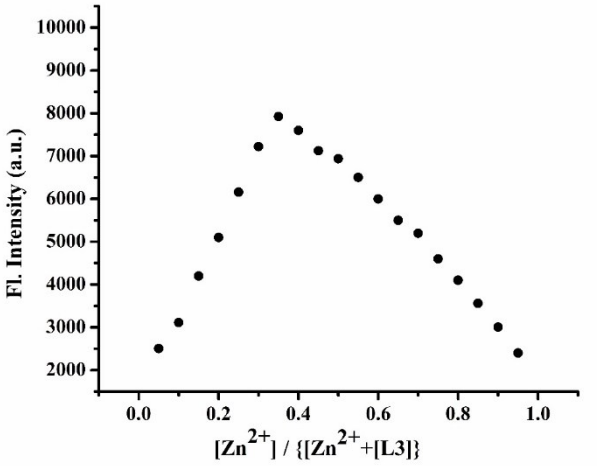

Figure S16c. Job's plot for stoichiometry determination of **[L3-Zn^{2+}]** complex, (λ_{ex} = 353 nm λ_{em} = 432 nm)

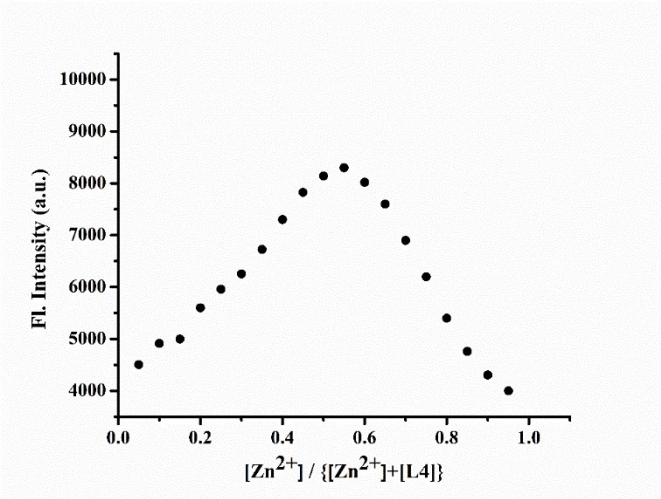

Figure S16d. Job's plot for stoichiometry determination of **[L4-Zn^{2+}]** complex, (λ_{ex} = 400 nm λ_{em} = 495 nm).

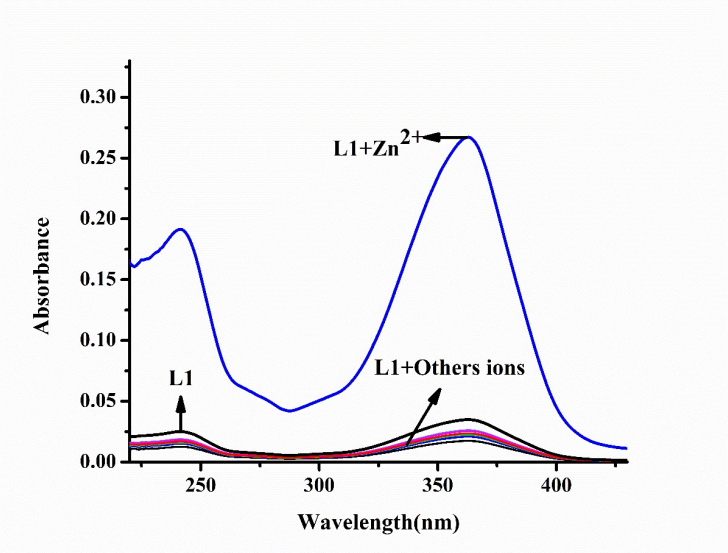

Figure S17a. UV-Vis selectivity of **L1** towards different metal ions.

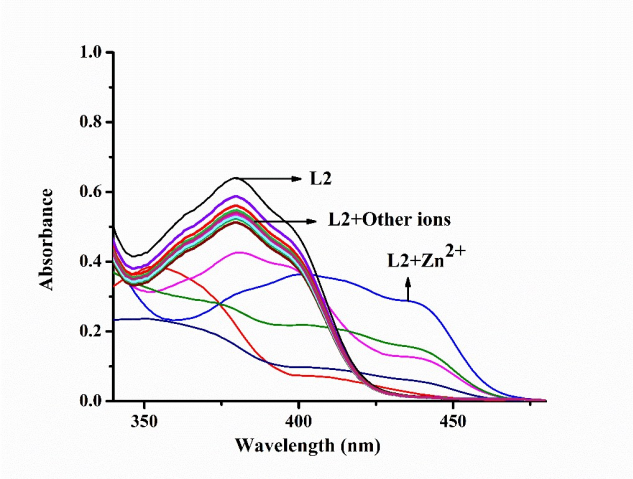

Figure S17b UV-Vis selectivity of **L2** towards different metal ions.

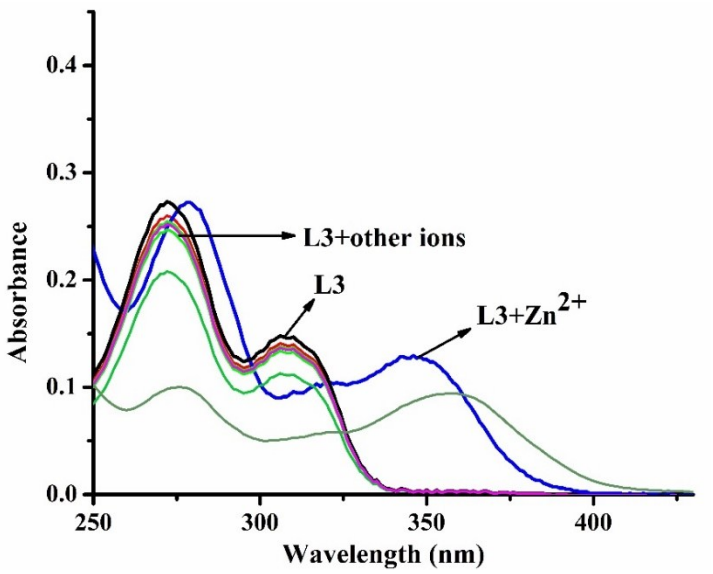

Figure S17c UV-Vis selectivity of **L3** towards different metal ions.

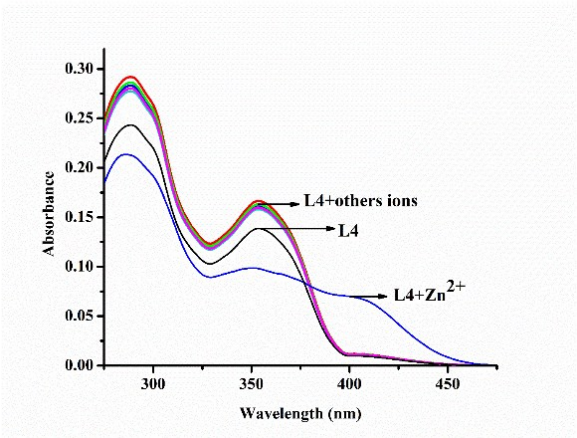

Figure S17d UV-Vis selectivity of **L4** towards different metal ions.

Table S1 Crystallographic parameters **L1, L2** and **L3.**

Molecules	**L1**	**L2**	**L3**
CCDC	1484206	1062760	1501269
Empirical formula	$C_{19}H_{25}N_3O$	$C_{19}H_{16}N_2O_2$	$C_{14}H_{12}N_2O_2$
Formula weight	311.42	304.34	240.26
Crystal system	Triclinic	Monoclinic	Monoclinic
Space group	P -1	P -1	P 21/C
Temparature	296 K	296 K	296 K
Wavelength	0.71073	0.71073	0.71073
a/Å	10.8682(5)	7.1822(10)	16.524(3)
b/Å	11.1818(6)	14.0258(18)	5.9394(12)
c/Å	16.0637(8)	15.7770(19)	13.232(2)
α/°	88.542(3)	89.987(9)	90
β/°	73.254(2)	90.007(10)	113.560(11)
γ/°	70.084(3)	77.128(10)	90
Volume/Å^3	1751.83(16)	1549.4(4)	1190.4(4)
Z	4	4	4
ρ_{calc} g/cm^3	1.181	1.305	1.341

μ/mm^{-1}	0.074	0.086	0.090
F(000)	672.0	640.0	504.0
F(000′)	672.23	640.27	504.22
Θmax	29.098	24.499	20.809
Index ranges (h,k,lmax)	14,15,21	8,16,18	16,5,13
Reflections collected	0.0749(5603)	0.1074(2244)	0.0525(915)
wR_2 (Reflection)	0.2493(8741)	0.2926(5122)	0.1502(1239)

Table S2a Selected bond lengths [Å] and angles [°] for **L1**

ATOMS	ATOMS LENGTH	ATOMS	ANGLE
O001 C00C	1.305(2)	C00J N003 C00V	121.68(18)
O002 C00M	1.291(2)	C009 N004 C00Z	120.99(16)
N003 C00J	1.322(2)	C009 N004 C00W	121.80(17)
N003 C00V	1.450(3)	C00Z N004 C00W	116.56(17)
N004 C009	1.356(2)	C00H N005 C00T	124.16(16)
N004 C00Z	1.447(3)	C00B N006 C00S	122.84(18)
N004 C00W	1.462(2)	C00D N3 C00Q	122.40(17)
N005 C00H	1.295(2)	C00D N3 C016	119.77(17)
N005 C00T	1.450(2)	C00Q N3 C016	117.83(18)
N006 C00B	1.373(2)	C00P N2 C00R	122.72(18)
N006 C00S	1.428(3)	N004 C009 C00L	122.33(17)
N3 C00D	1.365(2)	N004 C009 C00I	120.27(16)
N3 C00Q	1.448(3)	C00L C009 C00I	117.38(17)
N3 C016	1.536(4)	C00E C00A C00H	121.38(16)
N2 C00P	1.363(3)	C00E C00A C00C	117.85(16)
N2 C00R	1.426(3)	C00H C00A C00C	120.64(16)
C009 C00L	1.402(2)	N006 C00B C00U	119.35(19)
C009 C00I	1.429(3)	N006 C00B C00O	122.26(19)
C00A C00E	1.398(2)	C00U C00B C00O	118.38(19)
C00A C00H	1.407(3)	O001 C00C C00G	121.68(16)
C00A C00C	1.439(2)	O001 C00C C00A	119.75(15)
C00B C00U	1.389(3)	C00G C00C C00A	118.57(16)
C00B C00O	1.391(3)	N3 C00D C00G	121.82(17)
C00C C00G	1.387(2)	N3 C00D C00K	120.09(16)
C00D C00G	1.387(2)	C00G C00D C00K	118.09(16)
C00D C00K	1.422(3)	C00K C00E C00A	122.71(17)
C00E C00K	1.358(3)	C00J C00F C00N	119.36(17)
C00F C00J	1.391(3)	C00J C00F C00M	122.57(16)
C00F C00N	1.414(2)	C00N C00F C00M	118.07(16)
C00F C00M	1.441(3)	C00C C00G C00D	122.68(17)
C00I C00N	1.348(3)	N005 C00H C00A	122.96(16)
C00L C00M	1.395(3)	C00N C00I C009	120.72(16)
C00O C00Y	1.379(3)	N003 C00J C00F	124.02(18)
C00P C00X	1.382(3)	C00E C00K C00D	120.05(16)
C00P C012	1.389(4)	C00M C00L C009	123.08(18)
C00Q C014	1.501(3)	O002 C00M C00L	121.38(17)
C00R C00V	1.500(3)	O002 C00M C00F	120.53(17)
C00S C00T	1.514(3)	C00L C00M C00F	118.09(15)
C00U C013	1.370(3)	C00I C00N C00F	122.66(17)
C00W C010	1.482(3)	C00Y C00O C00B	119.9(2)

C00X C015	1.368(4)	N2 C00P C00X	122.7(2)
C00Y C011	1.372(4)	N2 C00P C012	119.4(2)
C00Z C017	1.497(4)	C00X C00P C012	117.9(2)
C011 C013	1.355(5)	N3 C00Q C014	113.96(19)
C012 C019	1.373(4)	N2 C00R C00V	110.88(18)
C015 C018	1.353(6)	N006 C00S C00T	114.49(17)
C016 C01A	1.340(5)	N005 C00T C00S	110.60(17)
C018 C019	1.376(6)	C013 C00U C00B	120.4(2)
		N003 C00V C00R	113.17(17)
		N004 C00W C010	115.32(19)
		C015 C00X C00P	120.8(3)
		C011 C00Y C00O	120.7(3)
		N004 C00Z C017	113.9(2)
		C013 C011 C00Y	119.6(2)
		C019 C012 C00P	120.5(3)
		C011 C013 C00U	121.1(3)
		C018 C015 C00X	120.9(4)
		C01A C016 N3	109.4(4)
		C015 C018 C019	119.6(3)
		C012 C019 C018	120.3(4)

Table S2b Selected bond lengths [Å] and angles [°] for **L2**

ATOMS	LENGTH	ATOMS	ANGLE
O001 C00A	1.372(6)	C00A O001 C00Z	117.6(5)
O001 C00Z	1.436(6)	C00C O002 C014	117.2(5)
O002 C00C	1.372(6)	C00R N003 N006	114.2(5)
O002 C014	1.433(6)	C00D N006 N003	113.0(5)
N003 C00R	1.288(6)	C00I N007 N008	113.6(5)
N003 N006	1.405(6)	C00T N008 N007	112.7(5)
O1 C00J	1.347(6)	C00Q C009 C00X	117.0(5)
O2 C00K	1.348(6)	C00Q C009 C00D	120.4(5)
N006 C00D	1.280(6)	C00X C009 C00D	122.6(5)
N007 C00I	1.284(6)	O001 C00A C00W	116.2(5)
N007 N008	1.403(6)	O001 C00A C011	124.2(5)
N008 C00T	1.279(6)	C00W C00A C011	119.6(5)
C009 C00Q	1.382(7)	C00H C00B C00V	116.8(5)
C009 C00X	1.398(7)	C00H C00B C00T	121.3(5)
C009 C00D	1.438(7)	C00V C00B C00T	121.9(5)
C00A C00W	1.377(7)	O002 C00C C00O	124.9(5)
C00A C011	1.384(8)	O002 C00C C00N	115.8(5)
C00B C00H	1.377(7)	C00O C00C C00N	119.3(5)
C00B C00V	1.402(7)	N006 C00D C009	123.5(5)
C00B C00T	1.445(7)	C00G C00E C013	124.2(5)
C00C C00O	1.376(8)	C00G C00E C00U	120.4(5)
C00C C00N	1.385(7)	C013 C00E C00U	115.4(5)
C00E C00G	1.417(7)	C010 C00F C00S	116.7(5)
C00E C013	1.419(8)	C010 C00F C00L	123.3(5)
C00E C00U	1.422(7)	C00S C00F C00L	120.0(5)
C00F C010	1.412(8)	C00J C00G C00E	118.8(5)
C00F C00S	1.416(7)	C00J C00G C00I	119.7(5)
C00F C00L	1.431(7)	C00E C00G C00I	121.5(5)

C00G C00J	1.391(8)	C00O C00H C00B	123.5(5)
C00G C00I	1.459(7)	N007 C00I C00G	121.8(5)
C00H C00O	1.375(7)	O1 C00J C00G	121.9(5)
C00J C00P	1.405(8)	O1 C00J C00P	117.8(6)
C00K C00Y	1.395(8)	C00G C00J C00P	120.2(6)
C00K C00L	1.397(7)	O2 C00K C00Y	117.7(6)
C00L C00R	1.450(7)	O2 C00K C00L	122.1(5)
C00M C00Y	1.345(8)	C00Y C00K C00L	120.2(5)
C00M C00S	1.414(8)	C00K C00L C00F	118.5(5)
C00N C00V	1.371(7)	C00K C00L C00R	120.3(5)
C00P C012	1.336(8)	C00F C00L C00R	121.2(5)
C00Q C011	1.384(8)	C00Y C00M C00S	121.0(5)
C00S C015	1.424(8)	C00V C00N C00C	121.2(5)
C00U C016	1.416(8)	C00H C00O C00C	118.9(5)
C00U C012	1.419(9)	C012 C00P C00J	121.3(6)
C00W C00X	1.367(7)	C009 C00Q C011	122.8(5)
C010 C019	1.359(8)	N003 C00R C00L	121.7(5)
C013 C018	1.352(8)	C00M C00S C00F	118.5(5)
C015 C01A	1.351(10)	C00M C00S C015	122.0(6)
C016 C017	1.362(10)	C00F C00S C015	119.5(6)
C017 C018	1.389(10)	N008 C00T C00B	123.9(5)
C019 C01A	1.381(10)	C016 C00U C012	121.7(6)
		C016 C00U C00E	120.6(6)
		C012 C00U C00E	117.7(5)
		C00N C00V C00B	120.4(5)
		C00X C00W C00A	121.2(6)
		C00W C00X C009	120.8(5)
		C00M C00Y C00K	121.7(6)
		C019 C010 C00F	122.5(6)
		C00A C011 C00Q	118.6(5)
		C00P C012 C00U	121.5(5)
		C018 C013 C00E	123.4(6)
		C01A C015 C00S	120.4(6)
		C017 C016 C00U	120.3(6)
		C016 C017 C018	120.2(6)
		C013 C018 C017	120.0(7)
		C010 C019 C01A	119.9(7)
		C015 C01A C019	120.9(7)

Table S2c Selected bond lengths [Å] and angles [°] for **L3**

ATOMS	LENGTH	ATOMS	ANGLE
N2 C14	1.277(7)	C14 N2 N2	113.3(6)
N2 N2	1.409(9)	C8 C13 C12	118.0(6)
C13 C8)	1.389(9	C8 C13 C14	122.8(6)
C13 C12	1.392(8)	C12 C13 C14	119.2(6)
C13 C14	1.444(8)	N2 C14 C13	121.7(6)
O1 C1	1.356(7)	C5 C6 C1	117.9(6)
O2 C8	1.350(7)	C5 C6 C7	118.8(6)
C6 C5	1.379(8)	C1 C6 C7	123.3(6)
C6 C1	1.399(8)	C7 N1 N1	113.1(6)
C6 C7	1.444(8)	C3 C2 C1	120.7(7)

N1 C7	1.286(7)	N1 C7 C6	121.3(6)
N1 N1	1.395(9)	O1 C1 C2	118.4(6)
C2 C3	1.356(8)	O1 C1 C6	122.0(6)
C2 C1	1.384(9)	C2 C1 C6	119.6(6)
C8 C9	1.377(9)	O2 C8 C9	118.4(6)
C5 C4	1.375(8)	O2 C8 C13	121.6(6)
C9 C10	1.357(9)	C9 C8 C13	120.0(6)
C12 C11	1.368(9)	C4 C5 C6	122.5(6)
C10 C11	1.386(9)	C10 C9 C8	120.5(7)
C4 C3	1.374(9)	C11 C12 C13	122.3(6)
		C9 C10 C11	121.3(7)
		C12 C11 C10	117.9(7)
		C3 C4 C5	118.1(7)
		C2 C3 C4	121.2(7)

Table S3a Results from TD-DFT calculations **L1**

Compound	**Electronic Transitions**	**Energy[a] (eV)**	**Wavelength (nm)**	**f[b]**	**Transitions involved**
L1	$S_0 \rightarrow S_1$	3.4093 eV	363.66 nm	0.0006	HOMO→LUMO
	$S_0 \rightarrow S_2$	4.1023 eV	302.23 nm	0.2140	HOMO-1→LUMO
	$S_0 \rightarrow S_3$	4.1805 eV	296.58 nm	0.0012	HOMO-2→LUMO
Ad1	$S_0 \rightarrow S_1$	2.5981 eV	477.22 nm	0.0237	HOMO→LUMO HOMO→LUMO+1
	$S_0 \rightarrow S_2$	2.7253 eV	454.95 nm	0.0095	HOMO→LUMO HOMO→LUMO+1
	$S_0 \rightarrow S_3$	3.1730 eV	390.75 nm	0.0333	HOMO-2→LUMO HOMO-1→LUMO

Table S3b Results from TD-DFT calculations **L2**

Compound	**Electronic Transitions**	**Energy[a] (eV)**	**Wavelength (nm)**	**f[b]**	**Transitions involved**
L2	$S_0 \rightarrow S_1$	2.1393 eV	579.55 nm	0.0011	HOMO→LUMO HOMO→LUMO+1
	$S_0 \rightarrow S_2$	3.3369 eV	371.56 nm	0.4415	HOMO-1→LUMO+1 HOMO→LUMO+1 HOMO-1→LUMO+2

	$S_0 \rightarrow S_3$	3.3604 eV	368.96 nm	0.2098	HOMO-1→LUMO HOMO→LUMO+1
Ad2	$S_0 \rightarrow S_1$	2.5832 eV	479.96 nm	0.2214	HOMO→LUMO HOMO→LUMO+1
	$S_0 \rightarrow S_2$	2.8781 eV	430.78 nm	0.0899	HOMO→LUMO HOMO→LUMO+1
	$S_0 \rightarrow S_3$	3.0297 eV	409.23 nm	0.0035	HOMO-2→LUMO HOMO-1→LUMO

Table S3c Results from TD-DFT calculations **L3**

Compound	**Electronic Transitions**	**Energy[a] (eV)**	**Wavelength (nm)**	**f[b]**	**Transitions involved**
L3	$S_0 \rightarrow S_1$	2.8344 eV	437.42 nm	0.0032	HOMO-1→LUMO HOMO→LUMO
	$S_0 \rightarrow S_2$	3.4892 eV	355.33 nm	0.3604	HOMO-3→LUMO HOMO-1→LUMO HOMO→LUMO
	$S_0 \rightarrow S_3$	3.5993 eV	344.46 nm	0.0000	HOMO-2→LUMO
Ad3	$S_0 \rightarrow S_1$	2.4341 eV	509.35 nm	0.1602	HOMO→LUMO
	$S_0 \rightarrow S_2$	2.6128 eV	474.52 nm	0.0156	HOMO-1→LUMO
	$S_0 \rightarrow S_3$	2.8735 eV	431.48 nm	0.0130	HOMO-1→LUMO+2 HOMO→LUMO+1 HOMO→LUMO+2

Table S3d Results from TD-DFT calculations **L4**

Compound	**Electronic Transitions**	**Energy[a] (eV)**	**Wavelength (nm)**	**f[b]**	**Transitions involved**
L4	$S_0 \rightarrow S_1$	2.2125 eV	560.37 nm	0.0010	HOMO→LUMO

	$S_0 \rightarrow S_2$	3.8393 eV	322.93 nm	0.1059	HOMO-1→LUMO HOMO→LUMO+1 HOMO→LUMO+3
	$S_0 \rightarrow S_3$	3.8715 eV	320.25 nm	0.6709	HOMO-2→LUMO HOMO-1→LUMO HOMO→LUMO+1
Ad4	$S_0 \rightarrow S_1$	2.5615 eV	484.02 nm	0.0978	HOMO-1→LUMO HOMO→LUMO
	$S_0 \rightarrow S_2$	2.7394 eV	452.59 nm	0.0366	HOMO-2→LUMO HOMO-1→LUMO HOMO→LUMO
	$S_0 \rightarrow S_3$	3.3833 eV	366.46 nm	0.0024	HOMO→LUMO+1